AFRL-RH-WP-TR-2017-0076

Synergistic Interactions of Neuroprotective and Neurotrophic Factors against Sleep Deprivation

Armando Soto
Victor T. Chan
Nicholas J. DelRaso
TSgt. Renell H. Capati
TSgt. Levaugh C. Grant
Bio-effects Division
Molecular Bio-effects Branch

Amy D. Walters
David A. Dixon
Amber Braddock
Henry M. Jackson Foundation
For the Advancement of Military Medicine

Jonathon Soto
Oak Ridge Institute for Science and Education
2729 Q Street
Wright-Patterson AFB OH 45433-5707
Nicholas V. Reo
Wright State University
Dayton, OH

Final Technical Report

March-2017

Air Force Research Laboratory
711th Human Performance Wing
Airman Systems Directorate
Bio-effects Division
Molecular Bio-effects Branch
WPAFB, OH 45433-5707

STINFO COPY

NOTICE AND SIGNATURE PAGE

Using Government drawings, specifications, or other data included in this document for any purpose other than Government procurement does not in any way obligate the U.S. Government. The fact that the Government formulated or supplied the drawings, specifications, or other data does not license the holder or any other person or corporation; or convey any rights or permission to manufacture, use, or sell any patented invention that may relate to them.

This report was cleared for public release by the 88th ABW Public Affairs Office and is available to the general public, including foreign nationals. Copies may be obtained from the Defense Technical Information Center (DTIC) (http://www.dtic.mil).

Synergistic interactions of neuroprotective and neurotrophic factors against sleep deprivation

(AFRL-RH-WP-TR-2017- 0076) has been reviewed and is approved for publication in accordance with assigned distribution statement.

SOTO.ARMANDO.1262578328 Digitally signed by SOTO.ARMANDO.1262578328 DN: c=US, o=U.S. Government, ou=DoD, ou=PKI, ou=USAF, cn=SOTO.ARMANDO.1262578328 Date: 2017.11.29 08:41:13 -05'00'

ARMANDO SOTO
Work Unit Manager
Molecular Bioeffects Branch

MILLER.STEPHANIE.A.1230536283 Digitally signed by MILLER.STEPHANIE.A.1230536283 Date: 2017.12.03 12:59:42 -06'00'

STEPHANIE A. MILLER, DR-IV, DAF
Chief, Bioeffects Division
Airman Systems Directorate
711th Human Performance Wing
Air Force Research Laboratory

This report is published in the interest of scientific and technical information exchange, and its publication does not constitute the Government's approval or disapproval of its ideas or findings.

REPORT DOCUMENTATION PAGE

Form Approved
OMB No. 0704-0188

1. REPORT DATE *(DD-MM-YYYY)*	2. REPORT TYPE	3. DATES COVERED *(From - To)*
30-03-2017	Final	May-2013 to Sep-2016

4. TITLE AND SUBTITLE
Synergistic interactions of neuroprotective and neurotrophic factors against sleep deprivation

5a. CONTRACT NUMBER

5b. GRANT NUMBER

5c. PROGRAM ELEMENT NUMBER

5. AUTHOR (S)
[1]Armando Soto, [1]Victor T. [1]Chan, [1]Nicholas J. DelRaso, [1]Renell Capati, [1]Levaugh Grant, [2]Amy D. Walters, [2]David Dixon, [2]Amber Braddock, [3]Jonathon Soto, [4]Nicholas V. Reo

5d. PROJECT NUMBER
H0FL

5e. TASK NUMBER
30

5f. WORK UNIT NUMBER
03/H0FL

7. PERFORMING ORGANIZATION NAME(S) AND ADDRESS(ES)
[1]Molecular Bioeffects Branch; [2]Henry M. Jackson Foundation for the Advancement of Military Medicine; [3]Oak Ridge Institute for Science and Education; 2728 Q street, Bldg. 837, WPAFB, OH 45433-5707; [4]Wright State University, Dayton, OH

8. PERFORMING ORGANIZATION REPORT NUMBER

19. SPONSORING/MONITORING AGENCY NAME(S) AND ADDRESS(ES)
Air Force Materiel Command
Air Force Research Laboratory
711th Human Performance Wing
Human Effectiveness Directorate
Bioeffects Division
Molecular Bioeffects Branch
Wright-Patterson AFB, OH 45433-5707

10. SPONSOR/MONITOR'S ACRONYM(S)
711 HPW/RHDJ

11. SPONSORING/MONITORING AGENCY REPORT NUMBER
AFRL-RH-WP-TR-2017-0076

12. DISTRIBUTION AVAILABILITY STATEMENT:
Distribution A: approved for public release; distribution unlimited. (PA Case No. 88ABW-2017-6069, 30 Nov 2017)

13. SUPPLEMENTARY NOTES

14. Abstract:
Sleep deprivation is one of the most common stressors that Airmen face during military missions. Exposure to this stressor will diminish performan increase the risk of make mistakes during critical assignments. Previous investigations have suggested that damaging brain effect of sleep deprivat may be caused by accumulation of reactive oxidant species, triggered by the decrease in the antioxidant defense and malfunction of the endoplasm reticulum (ER) molecular chaperones, and consequently, causing an increase in neuronal cell death. In this study the synergistic effects of two cytoprotective peptides ADNP-8 and CNTF-11 that were derived from known proteins protective proteins were tested against sleep deprivation cond Results of these investigations demonstrated that peptide treatments decreased the levels of corticosterone hormone after sleep deprivation. In add treatment with ADNP-8 or CNTF-11 restored glutathione peroxidase activity in frontal lobe. Furthermore, immunohistochemistry analysis performed hippocampal slices demonstrated that peptide treatment decreased neuronal cell death and increase hippocampal neurogenesis compared to sleep deprived subjects. Additionally, examination of ER molecular chaperones measurements using QRT-PCR demonstrated that gene expression of th chaperones was restored in most of the brain regions assisting tissue cells to reestablished homeostasis.

15. SUBJECT TERMS
Sleep deprivation, ADNP-8, CNTF-11, oxidative stress

16. SECURITY CLASSIFICATION OF:			17. LIMITATION OF ABSTRACT	18. NUMBER OF PAGES	19a. NAME OF RESPONSIBLE PERSON
U					A. Soto
a. REPORT	b. ABSTRACT	c. THIS PAGE	SAR	58	19b. TELEPONE NUMBER (*Include area code*)
U	U	U			N/A

Standard Form 298 (Rev. 8-98)
Prescribed by ANSI-Std

THIS PAGE INTENTIONALLY LEFT BLANK.

TABLE OF CONTENTS

Section **Page**

LIST OF TABLES

Table **Page**

LIST OF FIGURES

Figure **Page**

PREFACE

The studies were conducted at the Molecular Bio-effects Branch (RHDJ), Bio-effects Division (RHD), Airman Systems Directorate of the 711 Human Performance Wing of the Air Force Research Laboratory (AFRL/711 HPW/RHDJ), Wright-Patterson AFB, OH.

Funding for the execution of this project was provided by the Air Force Office of Scientific Research (AFOSR). Contractor employees were working under Cooperative Agreement with the Henry M. Jackson Foundation FA8650-15-2-6608.

All studies involving animals were approved by the Wright-Patterson Institutional Animal Care and Use Committee, and were conducted in a facility accredited by the Association for the Assessment and Accreditation of Laboratory Animal Care, International, in accordance with the Guide for the Care and Use of Laboratory Animals, National Research Council (2011). Studies were conducted under approved Air Force Research Laboratory Institutional Animal Care and Use Committee, animal protocol number F-WA-2013-0147-A.

THIS PAGE INTENTIONALLY LEFT BLANK

Synergistic Interactions of Neuroprotective and Neurotrophic Factors against Sleep Deprivation

Abstract:

Sleep deprivation is one of the most common stressors that an Airman faces during their military missions. Exposure to this common stressor will diminish performance and increase the risk of make crucial mistakes during critical operational assignments. Previous investigations have suggested that the damaging effects of sleep deprivation in the brain, may be caused by accumulation of reactive oxidant species, triggered by a decrease in the antioxidant defense and malfunction of the endoplasmic reticulum (ER) molecular chaperones, then consequently, causing an increase in neuronal cell death. During the first phase of this study (base line), we investigated the effects of 48, 72 and 96 h periods of sleep deprivation in the brain using a rat model. After exposure to sleep deprivation, oxidative stress measurements were performed on study termination samples from key regions of the brain and in blood serum using various biochemical assays, including corticosterone levels, lipid peroxidation, glutathione peroxidase activity and others oxidative stress markers to assess the damaging effects of acute sleep deprivation at each time point. In addition, metabolic profiling using nuclear magnetic resonance (NMR) analysis of blood serum was also performed. In the second phase of the study, the synergistic effects of nasal administration of two peptides: activity dependent neuroprotective protein-8 (ADNP-8) and ciliary neurotrophic factor-11 (CNTF-11), against sleep 96 h of deprivation were tested. During this phase of the study, animals were pretreated for three weeks before exposure to 96 h sleep deprivation conditions with a daily dose of ADNP-8 at the concentration of 15 µg/kg, CNTF-11 at concentration of 750 µg/kg and a mixture of the same concentrations of the two peptides ADNP-8 + CNTF-11, followed by an another daily treatment using the same peptides during the 96 hours (4 days) of sleep deprivation conditions. After exposure to sleep deprivation, serum corticosterone and oxidative stress measurements from six brain regions including prefrontal cortex, parietal cortex, thalamus, hippocampus, cerebellum and brain stem were taken and evaluated. Results of these investigations demonstrated that peptide treatments decreased the levels of corticosterone hormone after sleep deprivation, and that treatment with ADNP-8 or CNTF-11 restored glutathione peroxidase activity in frontal lobe. Furthermore, immunohistochemistry analysis performed in hippocampal slices demonstrated that peptide treatment decreased neuronal cell death and increased hippocampal neurogenesis. Additionally, examination of ER molecular chaperones measurements using QRT-PCR demonstrated that gene expression of the ER chaperones was restored in most of the brain regions assisting the cell to reestablished homeostasis.

1.0. Introduction:

Sleep deprivation is the most common stressor that the Airman is exposed during military missions. It has been hypothesized that acute sleep deprivation results in oxidative stress causing modifications in the brain resulting in neuronal cell damage. Generally, oxidative stress arises when oxygen free-radical production exceeds cellular antioxidant defense capabilities, resulting in cellular damage due to oxidative modifications of proteins, lipids and nucleic acids. Major cellular oxidants include reactive oxygen species (ROS) such as superoxide O_2-, hydrogen peroxide (H_2O_2) and reactive nitrogen species (RNS) including nitric oxide (NO) (1). Investigations have suggested that accumulation of reactive oxygen species happened during wakefulness, while removal of free radicals occurs during sleep (2). However, the hypothesis that sleep deprivation causes oxidative damage in the brain remains unproven.

The endoplasmic reticulum is a sub-cellular organelle comprised of a reticular membranous network that extends throughout the cytoplasm and is contiguous with the nuclear envelope. It is the site where all secretory and integral membrane proteins are folded and post-translational modified in ATP-dependent chaperone-mediated processes. In addition, the ER is the major signal-transducing organelle in the cell that continuously responds to environmental cues (3). Recent gene expression analyses showed that sleep deprivation induced HSPA5 and other chaperones of the endoplasmic reticulum (ER) that are involved in the degradation of misfolded proteins in the brain isolated from several species (10). As stress can result in accumulation of unfolded proteins, the ER initial response is to limit the amount of accumulating unfolded proteins by inhibition of protein translation, increased expression of molecular chaperones, enhancing degradation of misfolded proteins and restoring normal ER response critical for cell survival (11). Therefore, we surmise that the ER protects the cell by upregulating molecular chaperones genes expressed to proteins resulting in a coordinated activation of several pathways triggering the unfolded protein response (UPR) or endoplasmic reticulum (ER) stress response. Conversely, prolonged UPR activated signaling pathways can lead to apoptosis and cell death (11).

Small peptides originating from truncated endogenous proteins have been identified to have neuroprotective and neurotrophic activities. Investigations have demonstrated ADNP-8 was highly efficient cytoprotective peptide even at femtomolar concentration (4). In addition, ADNP-8 application experiments demonstrated remarkable neuroprotective activities capable of protecting neuronal cultures from diverse chemical stressors and toxicants including dopamine and 6-hydroxydopamine toxicity, buthioninesulfoximine toxicity, H_2O_2, oxygen-glucose deprivation, cyanide poisoning, NMDA excitotoxicity and kainic acid excitotoxicity (5). Treatments with ADNP-8 resulted in a significant increase in neuronal survival, as well as a reduction of degenerative morphological changes (6). ADNP-8 also has been shown as a neuroprotective agent in a mouse model of closed head injury (CHI) by reducing mortality and facilitates neurobehavioral recovery (7), as

well as providing long-term protection against the progressive deleterious effects of closed head injury (8).

CNTF-11 is derived from ciliary neurotrophic factor (CNTF), which has an important role in the regulation of neural stem cell self-renewal and differentiation, a process known as neuropoiesis (also known as adult neurogenesis). In the dentate gyrus, CNTF enhances differentiation of neural precursor cells into neurons (9). Investigations have demonstrated that continuous secretion of recombinant CNTF from a slow release device resulted in a robust improvement of cognitive performances and the stabilization of synaptic protein levels in a mouse model of Alzheimer's disease (12). Other investigations have showed that peripheral administration of an 11-mer peptide (representing the amino acid residues 146-156 of CNTF) restored cognition by enhancing neurogenesis and neural plasticity in the hippocampus and cerebral cortex in a mouse model of Alzheimer's disease (13). In addition, a tetrapeptide (GDDL, corresponding to the amino acid residues 147-150 of CNTF) also showed activity and improved cognition by enhancing neurogenesis and neural plasticity in the dentate gyrus (14).

The objectives of this investigation were to demonstrate key cellular events occurring marking adverse effects of sleep deprivation in the brain and to assess the effectiveness of the ADNP-8 and CNTF-11 in protecting the brain against the damaging effects caused by acute sleep deprivation. We hypothesize that using a combination of neuropoietic and neuroprotective peptides will not only effectively protect the brain against the adverse effects of sleep deprivation, but also demonstrate likely cognitive enhancing effects, this based upon our data determining specific cellular protein content associated with specific phenotypic cellular densities. This concept is based on the reasoning that while ADNP-8 will protect the brain against neuronal cell damage caused by sleep deprivation, combined together with CNTF-11, will stimulate neurogenesis that is an important compensatory mechanism occurring in the hippocampus as part of the brain responsible for learning and memory.

2.0. Material and Methods

2.1. Sleep deprivation platform development

For this study, we developed a sleep deprivation multi-platform setup over water bath system for rats. The system involves a water tank 5.5 ft diameter which includes 88 platforms (5 cm diameter X 20 cm high) (Fig 1A). The water level inside the tank is 2 cm below the surface of the platforms. Following this approach, the animals are placed on the small platform and when they enter into a deep sleep or rapid eye movement (REM), the animals will lose balance and fall in the water forcing them to awake and swim or climb onto a platform. The advantages of using this multi-platform system are that the animals can move freely from one platform to other platform over the water and have social interaction allowing better evaluation of the stress caused by sleep deprivation only,

therefore eliminating other possible confounding stressful effects that occur with isolation and restricted movement.

In addition to the sleep deprivation platform, a wide platform (3 x 3 ft dimensions) over water system was also developed (Fig. 1B). The purpose of building this platform was to expose the subjects to equivalent environmental conditions to lower exposure variation assure a better evaluation of the effects that sleep deprivation has in the tested animals.

A B

Fig.1 A) The sleep deprivation multi-platform over water system. B) The wide platform over water system. This platform system allows the animals to sleep and move freely.

2.2. Experimental groups and sleep deprivation conditions

2.2.1. Phase I: Effects of 48, 72 and 96 h sleep deprivation (Base Line Study)

A total 30 Sprague Dawley male rats 6-8 weeks old were divided into five experimental groups of six animals/group including Home Cage Control (HC), Wide Platform Control (WP), sleep deprived 48 hours (SD-48 h), sleep deprived 72 hours (SD-72 h) and sleep deprived 96 hours (SD-96 h). The HC animals remained in their cage in the same room with the sleep deprived group and the WP control. The WP group were placed on the wide platform located inside a tank. Animals on this platform can interact socially, sleep and move freely. The SD groups were exposed to sleep deprivation conditions using the novel sleep deprivation platform system for 48, 72 and 96 hours (Fig. 2). At each time point, animals form every experimental group were sacrificed and blood and brain tissue dissected to accurately collect prefrontal cortex, thalamus, parietal lobe, hippocampus, cerebellum and brainstem tissues (Table 1) to perform biochemical assays to measure oxidative stress and ER chaperone response (Table 2).

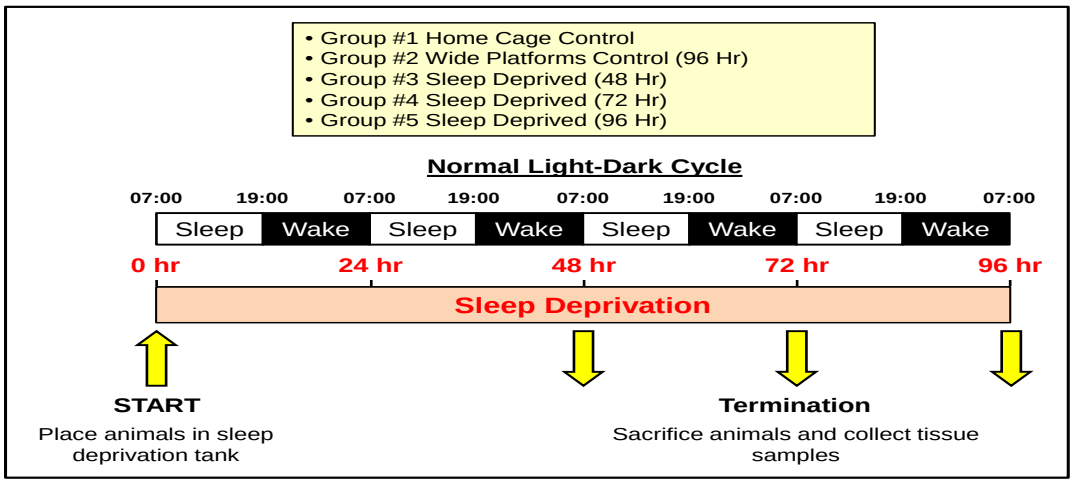

Figure 2. Experimental design representing the process during data generation for the sleep deprivation base line study. Light and dark describes the 12 h light-dark cycle that the animals were exposed during the study. Yellow arrows represent the time points for the period of the study and when animal were sacrificed for tissue collection.

Table 1. Brain regions collected and brief description of the executive and vegetative functionality of each brain region

Brain Region	Function
Frontal Lobe	Executive functions (working memory, reasoning, task flexibility, problem solving, planning and execution), attention, reward, motivation, and retention of long-term memories
Hippocampus	Memory consolidation and spatial navigation
Cerebellum	Motor control / learning, attention. language, fear / pleasure response
Parietal Lobe	Integration of sensory information, spatial awareness, and language processing
Thalamus	Relaying sensory / motor signals to cerebral cortex, regulation of consciousness, alertness, and sleep
Brainstem	Nerve connections of motor and sensory systems, maintaining consciousness, regulation of sleep cycle, heart rate, breathing, and eating

Table 2. Biochemical assays and endpoints.

Endpoint	Assay
Weight gain / loss	Body weight
Stress hormone	Serum corticosterone level
Oxidative stress	Protein oxidation; lipid peroxidation
Antioxidant defense	Glutathione peroxidase activity; superoxide dismutase activity
Unfolded protein response	Gene expression of endoplasmic reticulum chaperones

2.2.2. Phase II: Peptide treatments

To investigate the effectiveness of the neuropeptides ADNP-8 and CNTF-11 against sleep deprivation conditions, a total of 36 Wistar male rats 6-8 weeks old were divided into six experimental groups including, home cage control (HCC), wide platform control (WPC), sleep deprived (SD), sleep deprived-ADNP-8 (SD-ADNP-8), sleep deprived-CNTF-11 (SD+CNTF-11) and sleep deprived-ADNP-8+CNTF-11 (SD-ADNP-8+CNTF-11). The HCC animals remained in their cage in the same room with the SD and WP control group. The WPC group was placed on the wide platform located inside a tank. Animals on this platform can interact socially, sleep and move freely. The SD groups were placed in the sleep deprivation platform system and exposed to 96 h of sleep deprivation conditions (Table 3). The SD groups were pre-treated daily for three weeks before exposure to sleep deprivation conditions followed by a daily treatment during sleep deprivation exposure with an intranasal concentration of 15 µg/kg of activity dependent neuroprotective protein-8 (ADNP-8), 750 µg/kg of ciliary neurotrophic factor 11 (CNTF-11) and a mix of ADNP-8 and CNTF-11 at these same dose amounts. In addition, HCC, WPC and SD were also dosed with 765 µg/kg of a none-specific sequence amino acids to test that the sequence used in the peptides treatment for ADNP-8 and CNTF-11 are sequence specific (Table 3; Fig 3). Although ADNP-8 and CNTF-11 have not been used in sleep deprivation studies, they have shown activities against a wide variety of neurotoxic insults (5). Therefore, the doses of the peptides used in this experiment are based on the reports described in the literature. The biologically active dose of ADNP-8 used in this study has a sequence of eight amino acids including Asn-Ala-Pro-Val-Ser-Ile-Pro-Gln (NAPVSIP). For instance, it has been reported that a single dose up to 15 mg of ADNP-8 administered intranasally was safe and well-tolerated in humans (Gozes et al., 2005). For CNTF-11, an 11-mer fragment derived from CNTF included the amino acid sequence Val-Gly-Asp-Gly-Gly-Leu-Phe-Glu-Lys-Lys-Leu (VGDGGLFEKKL), which

retained the biological activity of the parent protein with no apparent side effects was used in a concentration described above.

Table 3. Experimental groups, schedule and peptide treatment concentrations

Group (6 animals/group)	Three weeks pretreatment	Four days treatment during sleep deprivation
1. Sleep deprived 96 h	Control AA's, 765 µg/kg/day	Control AA's, 765 µg/kg/day
2. Sleep deprived 96 h	ADNP-8, 15 µg/kg/day	ADNP-8, 15 µg/kg/day
3. Sleep deprived 96 h	CNTF-11, 750 µg/kg/day	CNTF-11, 750 µg/kg/day
4. Sleep deprived 96 h	ADNP-8 + CNTF-11/day	ADNP-8 + CNTF-11/day
5. Wide platform control	Control AA's, 765 µg/kg/day	Control AA's, 765 µg/kg/day
6. Home cage control	Control AA's, 765 µg/kg/day	Control AA's, 765 µg/kg/day

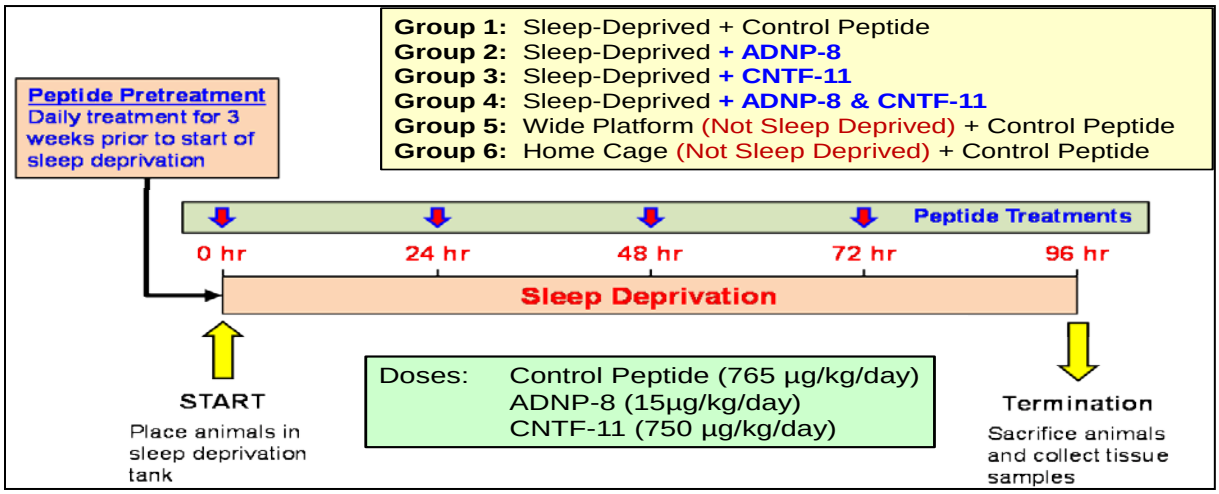

Figure 3. Graphic representation of the experimental design. Animals were pretreated daily for three weeks with peptides before exposed to sleep deprivation for 96 h. Yellow arrows indicate the beginning and end of the sleep deprivation period respectively. Red arrows indicate the four treatments with peptides during sleep deprivation exposure.

2.3. Brain sectioning and tissue collection

After 96 h of sleep deprivation, animals were sacrificed and brain sections were dissected including frontal lobe, parietal lobe, thalamus, hippocampus, cerebellum and brainstem. In addition, blood serum was also collected to evaluate corticosterone levels.

2.4. Assays and endpoints

Several biochemical test to evaluate stress, oxidative and antioxidant response were performed including corticosterone, protein oxidation, lipid peroxidation, superoxide dismutase, glutathione peroxidase and endoplasmic reticulum chaperones response. In addition, histochemical and immunohistochemical staining was completed using Fluoro-Jade staining, TUNEL assay and Doublecortin staining (DCX) to measure neuronal cell death, apoptosis and neurogenesis, respectively (Table 4).

Table 4: Assays and endpoints

Endpoint	Assay
Weight gain / loss	Body weight
Stress hormone	Serum corticosterone level
Oxidative stress	Protein oxidation; lipid peroxidation
Antioxidant defense	Glutathione peroxidase activity; superoxide dismutase activity
Unfolded protein response	Gene expression of endoplasmic reticulum chaperones
Neuronal death	Fluoro-Jade staining
Apoptosis	TUNEL assay
Neurogenesis	Doublecortin staining (DCX)

2.5. Weigh measurements

To evaluate the effects of sleep deprivation on body weight, animals from all experimental groups were weighted before and after 96 h exposure of sleep deprivation.

2.6. Corticosteroid measurements

Corticosterone is a steroid hormone produced in the cortex of the adrenal glands and is involved in regulation of energy, immune responses and stress response. Corticosterone levels were measured in blood serum collected from all animal groups using the corticosterone enzyme immunoassay kit (Arbor assays Cat No. K014-H1), following the manufacturing instructions. In brief, 5 µL of serum was mixed with 750 µL of assay buffer. A 50 µL mixed sample was loaded into a 96 well plate and 25 µL of corticosterone conjugate was added followed by 25 µL of corticosterone antibody. The plate was incubated at room temperature and moderately shaken for 1 h. After an hour incubation, plate was washed 3 times. Then, 100 µL of TMB substrate was added to each well followed by 30 min incubation at room temperature. Stop solution (50 µL) was added to each well. The plate was read at 450 nm absorbance.

2.7. Protein oxidation

Protein carbonyl was evaluated using the Protein Carbonyl Content Assay Kit (Sigma-Aldrich, Cat. No. MAK094), the kit measures the carbonyl content of samples from selected brain regions using the conversion of 2,4-dinitrophenylhydrazine (DNPH) to dinitrophenyl (DNP) hydrazone adducts, which can be detected spectrophotometrically at 375 nm. Briefly, 10 mg of brain tissue was homogenized in a tube containing 3-4 zirconium oxide grinding beads (2mm) using the Bullet Blender Gold (*Next Advance*, New York, USA) in 600 mL of homogenizing buffer (20 mM Tris-HCL, pH 7.5, 1 mM EDTA, 5 mM BHT, 1 mM DTT, 50 mM NaCl, 1% protease inhibitor and 0.25% peroxidase free Triton-X-100) for 2 min. The homogenate was centrifuged at 10,000 rpm for 10 min at 4 ˚C. The supernatant was transferred to a new tube and normalized to a 30 µg/mL concentration. A sample of 100 µL normalized supernatant was transferred to a tube containing 100 µL of DNPH solution and incubated at room temperature for 10 min. Then, 30 µL of 100% TCA (trichloroacetic acid) was added, vortexed and incubated in ice for 5 min and then centrifuged at 13,000 rpm for 2 min. The supernatant was discarded and the pellet was washed 2X with 500 µL of ice cold acetone, incubated at -20 ˚C for 5 min and then centrifuged at 13,000 rpm for 2 min. Using 200 µL of 5M guanidine was added and the sample was vortexed briefly to dissolve the pellet. Lastly, 100 µL of sample was added to designated wells and the plate was read at 375 nm.

2.8. Lipid peroxidation

Peroxidative damage of neuronal cell lipids was colorimetrically determined by measuring thiobarbituric acid reactive substances (TBARS) using the TBARS assay kit (Cayman Chemicals, Cat. No. 10009055). In brief, 25 mg of brain tissue was homogenized in a tube containing 3-4 zirconium oxide grinding beads (2 mm) using the Bullet Blender Gold in 250 µL of RIPA homogenizing buffer for 2 min. Homogenates of 100 µL aliquots were mixed with 100 µL of SDS (sodium dodecyl sulfate). Then, 4 µL of color reagent was added followed by incubation in boiling water (95-100 ˚C) for 1 h. To stop the reaction, samples were incubated in ice cold water bath for 10 min and then centrifuged for 10min at 1600 rpm at 4 ˚C. Plates were loaded with 150 µL of sample and read at 530 nm. Lipid peroxidation was calculated as µM of MDA-TBA adduct formed by MDA and TBA under high temperature and acidic conditions.

2.9. Superoxide dismutase

The amount superoxide dismutase (SOD) activity was measured using a SOD kit (Cayman Chemicals, Cat No. 706002). Overall, 25 mg of brain tissue was placed in 250 mL of homogenizing buffer (0.1 M HEPES buffer, pH 7.2; 1 mM EGTA, 210 mM mannitol, 70 mM sucrose) and homogenized using the bullet blender gold (described above). After centrifuging at 10,000 rpm for 10 min at 4 ˚C, each sample was further diluted 1:75 in homogenizing buffer. Plates were loaded with 10 µL sample and 200 µL of radical detector. To initiate the reaction, 20 µL of diluted xanthine oxidase was added followed

by moderate shaking for 20 min at room temperature. Finally, plates were read at 450 nm.

2.10. Glutathione peroxidase activity

Glutathione peroxidase (GPx) catalyzed reduction of hydroperoxides by reduced glutathione, which protects cells from oxidative damage. GPx activity was measured using the Glutathione Peroxidase Assay Kit (Cayman Chemicals, Cat. No. 703102) following manufacturing instructions. Briefly, 20 mg of brain tissue was homogenized in 250 µL of homogenization buffer (50 mM Tris-HCL, 5 mM EDTA, 1 mM DTT) using the Bullet Blender Gold (described above) to a final concentration of 0.084 mg protein from tissue/mL. The homogenized samples were spun at 10,000 rpm for 15 min at 4 ˚C and supernatant was collected. 20 µL of each normalized sample was mixed with 100 µL of assay buffer and 50 µL of a co-substrate mixture (NADPH), followed by the addition of 20 µL of GPx cumene hydroperoxide to start the reaction. Plates were read at 340 nm and readings were recorded every minute for 5 min to obtain at least 5 time points.

2.11. Unfolded protein response

Nine molecular chaperones mRNAs including CANX, CALR, HSP90AB1, HSP90B1, HSPA2, HSPA4, HSPA5, HSPB1 and PDIA4, representing cellular unfolded protein response elicited from the endoplasmic reticulum (ER) in response to sleep deprivation, were quantitated using the Brilliant II SYBR Green Real-time quantitative reverse transcription polymerase chain reaction (QRT-PCR) Kit (Agilent Technologies, Cat. No. 600834) according to manufacturing instructions. In general, total RNA was isolated from 30 mg of tissue using RNEasy Qiagen kit (Qiagen, Cat. No. 74106). A 6 µL aliquot containing 500 ng of total RNA was used for cDNA synthesis using Oligo DT primers at one cycle of 25 ˚C for 5 minutes, one cycle of 42 ˚C for 15 minutes, one cycle of 95 ˚C for 5 minutes, and 4 ˚C forever. cDNA synthesis was followed immediately by 10 separate QPCR reactions using specific primers (Table 5) . QPCR was performed on the Agilent Mx3005P (*Agilent Technologies*, Santa Clara, CA) at one cycle of 95 ˚C for 10 minutes followed by 40 cycles of 95 ˚C for 30 seconds/60 ˚C for 1 minute.

Table 5. Molecular chaperones primer sequence used to detect ER functionality. *ACTB is the Beta Actin housekeeping gene.

Gene I. D.	Forward primer	Reverse primer
CANX	5'-TTCACAACAGACTGGTCAACT-3'	5'-CCCAAGACAGGTGTATATGAAGA-3'
CALR	5'-TTGTCCTTCATCTGCTTCTCTG-3'	5'-TTTGCTGTACTGGGCTTAGAC-3'
HSP90AB1	5'-GCGAGACACATACTCTGACAG-3'	5'-ACAAGAAATTTTATGAGGCATTCTCT-3'
HSP90B1	5'-AAACAAAACTACAGCAAGATCCA-3"	5'-ACGGGCAAGGACATCTCTA-3'
HSPA2	Qiagen Quantitect Proprietary	Qiagen Quantitect Proprietary
HSPA4	5'-GGAGCAGCATGGTTTTTGG-3'	5'-GCAGTGTGCAATCTTATCACC-3'
HSPA5	5'-CTTCTCTCCCTCTCTCTTATCCA-3'	5'-GTGACTGTACCAGCTTACTTCA-3'
HSPB1	5'-ACAGGGAAGAGGACACCAA-3'	5'-GGAGATCACTGGCAAGCAC-3'
PDIA4	5'-CAAATTGCTTGCAGTGTCCAC-3'	5'-GGAAGTTAAGGAAGAAAATGGTGT-3'
*ACTB	5'-GGCATAGAGGTCTTTACGGATG-3'	5'-TCACTATCGGCAATGAGCG-3'

2.12. Brain perfusion

The brain perfusion was accomplished using a Perfusion Two^{TM} System (myNeurolab, Leica Microsystems) following manufacture recommendations. Overall, animals were transcardially perfused via the right ventricle with 400 mL of 10% sucrose to flush blood from tissues, followed by 300 mL of perfusion fixative containing 4% paraformaldehyde to fix the tissue. The pressure of the perfusion pump was maintained between 250-300 mmHg and 150-200 mmHg during the wash and fixative period, respectively. After perfusion, whole brains were post-fixed overnight in a solution containing 4% formaldehyde and 20% sucrose.

2.13. Fluoro-Jade staining

Coronal sections representing diverse parts of the brain were cut using a freezing sliding microtome (*Avantik* model QS[11]) and stained using the Fluoro-Jade C Kit (Chemicon International, Cat. No. AG325) according to manufacturing instructions. Briefly, brain sections (20 µm thick) were mounted on 2% gelatin coated slides and then air dried on a slide warmer at 50 °C for at least half an hour. The slides were then dehydrated and rehydrated in ethanol solutions (50%-70%-100%-70%-50%) for one minute each. This was followed by a 1 minute wash in distilled water. The slides were then incubated in 0.06% potassium permanganate solution for 10 min, preferably on a shaker table to insure consistent background suppression between sections. Following a 1-2 minutes water rinse, the slides were then transferred for 30 min to a 0.0008% solution of Fluoro-Jade C dissolved in 0.1% acetic acid vehicle with Hoeschet stain. After 30 min in the staining solution, the slides were washed 3X, one minute each cycle with distilled water. Excess water was drained onto a paper towel, and the slides were then incubated in a dark chamber overnight at 37 °C. The dry slides were cleared by immersion in xylene for

at least a min 3X before cover-slip mounting with DPX ((Sigma), a non-aqueous non-fluorescent plastic mounting media. These samples were allowed to dry in the dark overnight. After drying, the tissue was then examined using an epifluorescent microscope with blue excitation light (450-490 nm) using a barrier filter that allows passage wavelengths of 525 nm emission.

2.14. Tunel assay

Tunel (terminal deoxynucleotidyltransferase) assay is a staining method that labels the terminal end of nucleic acids and is commonly used to detect DNA fragmentation resulting from progression DNA digestion initiated by apoptotic signaling cascades. The assays depend on the presence of nicks in the DNA, which can be identified by the terminal deoxynucleotidyltransferase (TdT) enzyme that will catalyze the addition of dUTPs that are labeled with a fluorescent marker or biotin-dUTP. Briefly, coronal sections representing diverse parts of the brain were cut using a freezing sliding microtome (*Avantik* model QS[11]) and stained using the ApopTag Plus Peroxidase *in Stu* Apoptosis Detection Kit from Millipore. Brain sections 10 µm thick were mounted on 2% gelatin coated slides and then air dried on a slide warmer at 50 ˚C for at least half an hour. Slides were post fixed in pre-cooled Ethanol: Acetic Acid (2:1 volume ratio) at -20 ˚C for 5 min, then washed twice in 1X PBS for 1 min. Endogenous peroxide was quenched using a solution of 3% hydrogen peroxide in 1X PBS for 5 min, then slides were rinsed in two changes of 1xPBS for 5 min. Pipetting 75 µl/5 cm^2 area using equilibrium buffer was added directly to the tissue, and incubated for 10 sec. Liquid was decanted, and 55µl/5cm^2 area was added of working strength TdT enxyme. Slides then were incubated in a humidified chamber in the dark for 1 h at 37 ˚C. Slides were then submerged in 100 ml of stop/wash buffer for 10 min, and washed by submerging in three changes of 100ml each of 1X PBS for 1 min each. Application of 65 µl/5 cm^2 area of Anti-Digoxigenin Peroxidase conjugate was added to each slide, and incubated for 30 min in a humidified chamber in the dark at room temperature. Slides were then washed in four changes of 100 ml each 1X PBS for 2 min. Peroxidase substrate was added at 75 µl/5 cm^2 area, and tissue was stained for 4.5 min. Slides were washed using three changes of RO water for 1 min each, then incubated in RO water for 5 min at room temperature. Slides were counterstained with 0.5% Methyl Green from Sigma for 10 min at room temperature, then washed in three changes of RO water, dipping each slide 10 times followed by 30 sec of agitation. The tissue was then cleared by washing the slides in three changes of 100% N-Butanol, dipping each slide 10 times in the first wash, followed by 30 sec of incubation in the remaining washes. Tissue was then dehydrated by moving the slides through three changes of Xylene, two minute incubation in each wash. Slides were gently tapped to drain, and mounted under a glass coverslip using DPX from Sigma. Slides were dried overnight in the dark, then the tissue was examined using a confocal microscope under bright field.

2.15. Doublecortin (DCX)

Doublecortin (DCX) is a staining method that labels immature neurons, and is paired with DAPI (nuclear stain). Coronal sections representing diverse parts of the brain were cut using a freezing sliding microtome from *Avantik* model QS[11]. Briefly, brain sections 20 µm thick were mounted on 2% gelatin coated slides and then air dried on a slide warmer at 50 ˚C for at least half an hour. Slides were washed three times in 1X PBS for 5 min, and blotted on a paper towel to dry. Tissue was blocked for 1 h at room temperature in a humidified chamber with a blocking solution of 2% Donkey Serum 3% BSA and 0.3% TritonX in 1X PBS. The tissue is gently blotted on a paper towel to dry, and tissue is incubated in Goat Anti-Doublecortin from Santa Cruz at a dilution of 1:100 in 0.3% TrintonX 1X PBS, and allowed to incubate overnight in a humidified chamber at 4 ˚C. When incubation is complete, the excess antibody removed and blotted off tissues, and slides are washed three times for 5 min in 0.3% TritonX 1xPBS. Slides were then incubated in Donkey Anti-Goat FITC from Jackson Immuno Research at a 1:150 dilution in 2% donkey serum, 3% BSA 0.3% TritonX 1X PBS for 2 h in the dark in a humidified chamber at room temperature. After incubation, the excess of antibody is removed by shaking the slide over paper towels, then slides are washed by submerging in three changes of 100ml each of 0.3% TritonX 1X PBS for 5 min each, followed by submerging three changes of 100ml each 1X PBS for 1 min each. Slides are blotted in a stock of paper towels to dry, then mounted with Gold Anti-Fade DAPI from Molecular Probes and allowed to cure overnight at room temperature while protected from light. After drying, the tissue was then examined using a confocal microscope with filters for 405 nm and 488 nm absorbance/emission light respectively.

2.16. Nuclear Magnetic Resonance (NMR) spectroscopy

On the day of NMR analysis, serum samples were thawed and centrifuged (5000 rpm for 10 min) to remove any particulate matter. A 0.550 mL aliquot of serum was transferred into a 5 mm NMR tube along with 0.150 mL of 9 mM trimethylsilylpropionic (2,2,3,3 D4) acid (TSP) in D2O. TSP is added as a chemical shift and concentration reference. Samples were analyzed using 1H NMR spectroscopy conducted on a Varian Inova 600 NMR spectrometer. NMR spectra were acquired at 600 MHz and 25 °C using a pulse sequence designed to suppress the large proton resonance from water and the broad resonances from macromolecules. The proteins and lipids contained in serum give rise to broad components in the spectrum, which make it difficult to accurately analyze the sharper signals from small metabolite molecules. Therefore, we used a pulse sequence that incorporates solvent suppression in combination with a spin-echo detection method (cpmg spin-echo). The solvent suppression portion minimizes the signal from water and the spin-echo sequence allows delay of the signal detection period to minimize the broad NMR signals. Water suppression is achieved using the first increment of a NOESY pulse sequence, which incorporates saturating irradiation (on-resonance for water) during the relaxation delay (2 sec) and the mixing time (38 msec). The time-to-echo (TE) for the acquisition of data was 68 msec. Data was signal averaged (256 transients) using an interpulse delay of 7.106 sec. These spectra provide a metabolite profile of the serum, which was used as input for multivariate data analyses. Multivariate data analyses were

conducted on binned, scaled spectral data using MATLAB software. Binned NMR data were scaled to a chosen reference dataset by subtracting each bin value from the mean value for the corresponding bin in the reference data, then dividing this value by the standard deviation of the reference data (auto-scaling). The reference data for auto-scaling was chosen to emphasize specific effects.

2.16.1. Multivariate NMR Data Analyses.

Multivariate data analyses were conducted on binned, autoscaled spectral data using MATLAB. Autoscaling is a procedure that is used to scale spectral peak intensities such that changes in signal intensities can be compared between peaks of varying intensity. Here a group of spectra is chosen as a reference (i.e., control group) and peak intensities are scaled to the mean intensity for each peak (or bin) in the reference group. These data are further normalized to the standard deviation of the intensities for the reference bins. Autoscaling ensures that a proportional change in intensity for a strong signal (i.e., 20% increase) is equivalent to the same percentage change in a weak signal. When analyzing the multivariate data we will typically choose different experimental groups to serve as "reference" for autoscaling and examine which procedure provides the best results.

Unsupervised Principal Component Analysis (PCA): PCA is a pattern recognition analysis that is unsupervised (experimental groups are not identified to the analysis software a priori). Metabolite profiles among the three experimental groups were visualized using PCA and scores plots of the first two PCs (PC1 vs. PC2). We constructed various autoscaled datasets of the binned NMR spectra using (1) all groups as reference, (2) all control rats as reference, and (3) the sleep deprived group as reference. No matter which way we chose to autoscale the data, PCA scores plots show complete separation between all three experimental groups. The best result, however, was achieved when the data were autoscaled using the sleep-deprived (SD) group as reference (this includes all time points in the group).

Supervised Analysis. Orthogonal Projections onto Latent Structures Discriminant Analysis (OPLS-DA) was used to classify data and identify salient features that allow class separation. In order to apply OPLS-DA, spectral data are collected into a matrix of variables or bins (X) and a vector of categorical labels (Y), representing the effects. Statistical Evaluation of OPLS Results. The OPLS model was evaluated on its predictive ability, using the Q^2 (coefficient of prediction) metric. Q^2 was calculated as follows:

$$Q^2 = 1 - \frac{PRESS}{SSY} = 1 - \frac{\sum_{i=1}^{n} e_i^{\,2}}{\sum_{i=1}^{n} (y_i - \bar{y}_i)^2} = 1 - \frac{\sum_{i=1}^{n} (y_i - \hat{y}_i)^2}{\sum_{i=1}^{n} (y_i - \bar{y}_i)^2}$$

where PRESS is the Predicted REsidual Sum of Squares calculated as the residual e between the predicted and actual Y (class labels) during a leave-one-out cross-validation

approach, SSY is the Sum of Squares for y is the y mean across all samples, and $\hat{y}_i$ is the y value for sample i. As Q^2 approaches unity, the more predictive capability the model exhibits. A Q^2 value less than zero indicates that the model has no predictive power. A permutation test was performed to evaluate the significance of the Q^2 metric. The test involved repeatedly permuting the data labels and re-running the discrimination analysis, resulting in a distribution of the Q^2 scores (Rozman and Doull 1998). The Q^2 from the correctly labeled data is then compared to the distribution to determine the significance of the model at a specified alpha (set herein at $\alpha = 0.01$). As a secondary validation of an OPLS binary model we used a receiver operator characteristic (ROC) curve and calculated the area under the curve (AUC). The significance of this AUC value was evaluated using the same permutation procedure as described above.

Variable selection (salient bins) from OPLS-DA was also statistically evaluated. The bin loadings, commonly referred to as coefficients, were compared to calculated null distributions in order to select for significance. The null distribution for each bin was determined by refitting the OPLS model to datasets in which each bin was independently and randomly permuted to remove any correlation between it and the control/treatment groups. The true OPLS model loading was then compared to the resulting null distribution of loadings, and values in the tail (greater than 99.5% or less than 0.5% of the null distribution; corresponding to alpha = 0.01) were assumed to contribute significantly to the model. The permutation was initially repeated 500 times for each bin and those near-significant loadings (greater than 92.5% or less than 7.5% of the null distribution; corresponding to alpha = 0.15) were selected for 500 additional permutations (total 1000). The salient spectral resonances were assigned to metabolites using Chenomx 5.1 software, on-line NMR databases (i.e., hmdb.ca, mmcd.nmrfam.wisc.edu, etc.), and by "spiking" samples with known compounds, if necessary.

2.17. Statistical Analysis

For the biochemical assays, each animal sample was tested in triplicate, the average of n=6 animals/group was used for statistical analysis using student t-test with a $p \leq 0.05$. For immunohistochemistry analysis, the number of dead, apoptotic or new cells formed were assessed from ten 10X microscope fields from different areas of each slice, images taken for a total of 30 fields/brain region/animal (n=6). For each animal the total number of cells was averaged across the fields resulting in average # of neurons/field of view. These averages were used for statistical analysis using student t-test with a $p \leq 0.05$.

3.0. RESULTS

3.1. Phase I: Effects of 48, 72 and 96 h sleep deprivation

3.1.1. Differences on weight. To determine changes in body weight, animals from all experimental groups were weighed before and after exposure to sleep deprivation. Results from these measurements indicated a significant ($p \leq 0.05$) increase on body weight of wide platform and cage control animal groups while 96 h sleep deprivation (SD 96 h) group indicated a significant ($p \leq 0.05$) decrease. No significant differences on SD 48 and 74 h were observed (Fig.4).

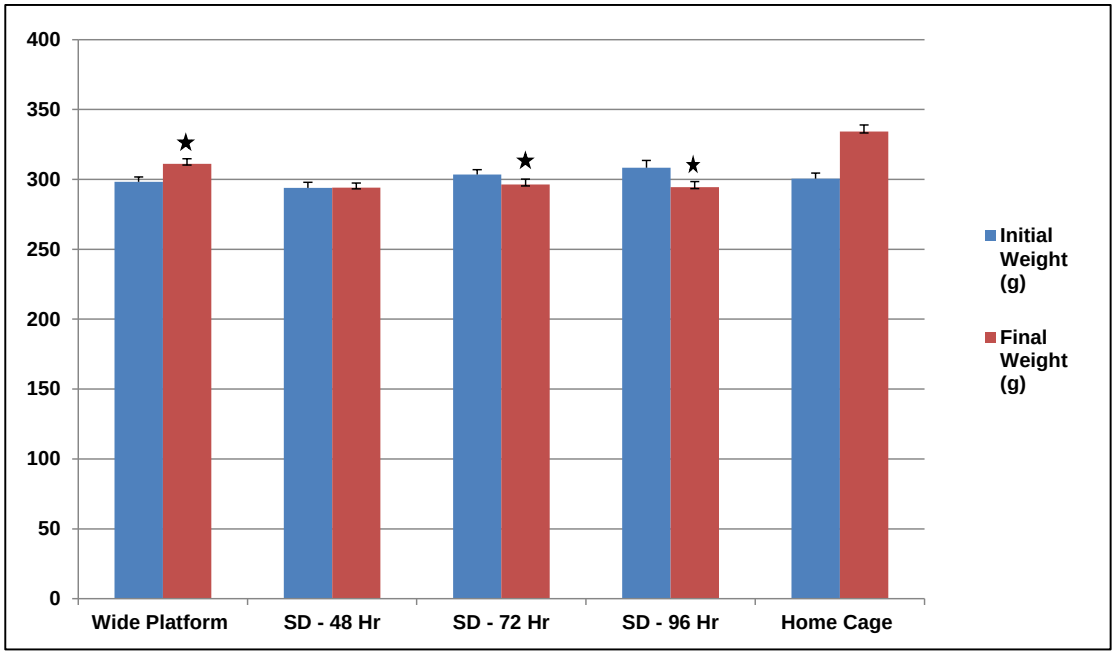

Figure 4. Representation of animal weights before and after exposure to sleep deprivation conditions. ★Significant difference ($p \leq 0.05$) before and after sleep deprivation.

3.1.2. Corticosterone levels

Corticosterone is a steroid (stress) hormone produced in the cortex of the adrenal glands and is involved in regulation of energy, immune responses and stress response. Corticosterone levels were measured on blood serum collected from all animal groups. Results from these analysis indicated a significant increase ($p \leq 0.01$) on corticosterone levels from sleep deprived animals from SD 48 h, SD 72 h and SD 96 h groups compared to wide platform control group (Fig. 5). No significant differences were observed on HC group.

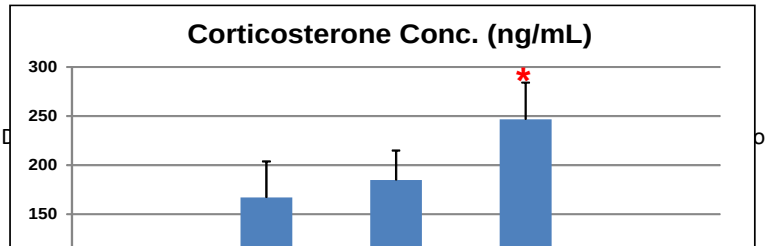

o 88ABW-2017-6069, 30 Nov 2017)

Figure 5. Representation of corticosterone level in blood serum.*Significant difference ($p \leq 0.01$) compared to wide platform control.

3.1.3. Lipid Peroxidation

Lipid peroxidation represent the oxidative degradation of lipids in which free radicals (hydroxyl radical, superoxide anion, hydroxyl anion, and oxide anion) steal electrons from lipids in cell membrane causing cell damage or oxidative stress. The end products of lipid peroxidation are reactive aldehydes including malondialdehyde (MDA) and hydroxynonenal (HNE). On this study, we used a TBARS assay (thiobarbituric acid) that reacts with MDA to yield a measurable fluorescent product that allows the measurement of lipid peroxidation in selected brain regions. Increased concentration of MDA representing the amount of lipid peroxidation was observed, in the parietal (SD-72 h) and hippocampal brain regions of animals after 48 and 72 h sleep deprivation compared to wide platform controls (table 6) indicating a possible increase in neuronal death. It was also observed a significant decrease ($p \leq 0.05$) in MDA concentration after 96 h sleep deprivation in the cerebellum, parietal and brain stem, after 96 h stress. The possible reason for the decrease in lipid peroxidation after 96 h could be related to a great number of neurons having already died and reabsorbed by microglia. However, histology studies including Fluoro-Jade staining and tunnel assay are necessary to confirm neuronal death. Unfortunately, for this phase of the study, immunohistochemistry analysis were not completed.

Table 6. Effect of sleep deprivation on brain region lipid peroxidation, measured by the concentration of MDA. *Statistical significant ($p \leq 0.05$) compared to WP-control group.

Group	Frontal (MDA µM)	Cerebellum (MDA µM)	Parietal (MDA µM)	Hippocampus (MDA µM)	Thalamus (MDA µM)	Brainstem (MDA µM)
SD-48 h	28±2	19±2	22±2	*21±1	21±2	15±4
SD-72 h	28±3	20±1	*23±1	*27±3	25±2	15±3
SD-96 h	16±2	*14±2	*12±1	18±4	18±2	*13±1
HC-control	25±3	18±2	17±1	13±2	25±2	16±2
WP-control	20±3	21±1	18±1	15±1	20±2	18±2

3.1.4. Protein Oxidation

Reactive oxygen species (ROS) including superoxide and hydrogen peroxide are continuously produced during metabolic processes. Excess of ROS can lead to cellular injury in the form of damaged DNA, lipids and proteins. Cellular proteins are subjected to oxidative stress and depending on the ROS present, the damage to the protein may take the form of nitration or oxidation of various amino acids residues. In this study, we used the protein carbonyl assay to measure protein oxidation for evaluation of oxidative stress response to sleep deprivation. Levels of dinitrophenyl hydrazone adduct representing the concentration of protein carbonyl oxidation are shown in Table 7. Results of this investigation indicated a significant ($p \leq 0.01$) increase in protein oxidation levels in frontal and cerebellum after 96 h sleep deprivation. The parietal lobe and hippocampus also displayed a significant increase ($p \leq 0.05$) in lipid peroxidation following 48 h sleep deprivation. Unexpectedly, HC-control as well displayed a significant increase ($p \leq 0.01$) in the frontal lobe compared to WP-control. In addition, the SD-48 h and HC-control in the cerebellum displayed a significant decrease ($p \leq 0.05$) in lipid peroxidation compared to WP-control. The reason for this discrepancy in the cerebellum could be that this is a large brain region and has different areas with each area representing diverse functionality.

Table 7. Protein oxidation values after sleep deprivation conditions. *Indicates significant increase compared to WP-control group. *****Indicates significant decrease compared to WP-control.

Group	Frontal (nmol)	Cerebellum (nmol)	Parietal (nmol)	Hippocampus (nmol)	Thalamus (nmol)	Brainstem (nmol)
SD-48 h	0.66±0.30	*****0.49±0.06	*0.66±0.31	*0.69±0.19	0.64±0.16	0.28±0.03
SD-72 h	0.68±0.11	0.57±0.2	1.0±0.90	0.34±0.10	0.46±0.23	0.37±0.11
SD-96 h	*2.07±0.66	*3.0±0.56	0.41±0.11	0.32±0.05	0.64±0.13	0.33±0.03
HC-Control	*2.42±0.90	*****0.55±0.08	0.33±0.05	0.32±0.03	0.48±0.07	0.30±0.07
WP-control	0.63±0.04	0.73±0.14	0.37±0.05	0.35±0.09	0.44±0.21	0.40±0.21

3.1.5. Glutathione Peroxidase (GPx) Activity

GPx plays an important role in the protection of organisms from oxidative damage. GPx converts reduced glutathione (GSH) to oxidized glutathione (GSSG), while reducing lipid hydroperoxides to their corresponding alcohols or free hydrogen peroxide to water. Glutathione reductase then reduces GSSG to GSH to complete the cycle. Therefore, low levels of GPx activity under stress conditions could be correlated with high free radical accumulation in the cell that might lead to neuronal cell death. After 48 h sleep deprivation (SD-48 h), all the brain regions, with the exception of parietal and brainstem, displayed a significant increase ($p \leq 0.05$) in GPx activity compared to WP-control group (Table 8). Although not a significant increase, parietal and brainstem also displayed some increase in GPx at the SD-48 h. Parietal lobe also exhibited a significant decrease ($p \leq 0.05$) in GPx activity levels after 96 h sleep deprived. Taken together, the data suggest that GPx activity increase during the first hours of sleep deprivation in the effort to protect the cells against oxidative stress, followed by a gradual decrease, reaching the lowest levels at 96 h of sleep deprivation (SD-96 h).

Table 8. GPx activity in different brain regions after sleep deprivation conditions. * Indicates significant difference compared to WP-control group. *****Indicates a significant ($p \leq 0.05$) decrease compared to WP-control.

Group	Frontal (nmol/min/ml)	Cerebellum (nmol/min/ml)	Hippocampus (nmol/min/ml)	Parietal (nmol/min/ml)	Thalamus (nmol/min/ml)	Brainstem (nmol/min/ml)
SD-48 h	*64±11	*134±25	*78±11	81±11	*98±11	149±21
SD-72 h	50±19	93±24	60±8	76±13	85±17	129±16
SD-96 h	28±13	77±19	44±10	*60±10	62±16	103±16
HC-control	46±16	98±11	49±4	87±10	83±21	116±20
WP-control	38±19	100±17	51±10	77±11	80±20	122±17

3.1.6. Superoxide dismutase activity test

Superoxide dismutases (SOD) are metalloenzymes that catalyze the dismutation of superoxide radical to hydrogen peroxide (H_2O_2) + molecular oxygen (O_2) and consequently provide an important defense mechanism against superoxide radical toxicity. Activity of superoxide dismutases was measured to evaluate the antioxidant response of the collected brain regions after sleep deprivation conditions. Results of frontal lobe indicated a significant ($p \leq 0.001$) decrease in SOD activity in all the sleep deprivation conditions compared to WP-control. Hippocampus, parietal and brain stem regions also displayed a significant ($p \leq 0.001$) decrease in SOD activity after 96 h sleep deprivation. Brainstem also showed a significant ($p \leq 0.02$) decrease in SOD activity after 48 h sleep deprivation and in the HC-control group. Overall, we can suggest that sleep deprivation reduced SOD activity after sleep deprivation, and the frontal cortex is the part of the brain that seems the most affected by this stressor. In addition, SOD activity in cerebellum and thalamus seem not to be affected by this stressor (Table 9).

Table 9. Effects of sleep deprivation in SOD activity in diverse parts of the brain. *****Indicate significant ($p \leq 0.001$) decrease and *****Indicate significant increase in SOD activity compared to WP-control group

Group	Frontal (Units/mL)	Cerebellum (Units/mL)	Hippocampus (Units/mL)	Parietal (Units/mL)	Thalamus (Units/mL)	Brainstem (Units/mL)
SD-48 h	*****68±11	97±5	90±11	71±16	77±17	*****81±19
SD-7 h	*****54±12	85±16	96±18	71±21	92±25	91±38
SD-96 h	*****40±12	80±15	*****54±7	*****55±8	54±14	*****57±8
HC-Control	143±19	100±16	117±28	*****124±13	67±7	*****83±24
WP-Control	126±21	91±16	97±9	92±18	73±	112±18

.

3.1.7. Endoplasmic reticulum (ER) molecular chaperones gene activation after 48, 72 and 96 h sleep deprivation

The unfolded protein response (UPR) is a cellular stress response that is activated in response to an accumulation of unfolded or misfolded proteins in the lumen of the endoplasmic reticulum (ER). The UPR has three aims after a significant cellular stress: i) initially to restore normal function of the cell by slowing down protein translation, ii) degrading misfolded proteins and iii) activating the signaling pathways that lead to increasing the production of molecular chaperones involved in protein folding. If these objectives are not achieved within a certain time lapse, or the disruption is prolonged, the UPR activities trends towards aiding in apoptosis. In this study, we used QRT-PCR to evaluate the level of expression of nine molecular chaperones genes (CANX, CALR, HSP90AB1, HSP90B1, HSPA2, HSPA4, HSPA5, HSPB1 and PDIA4) involved in ER response to sleep deprivation. The molecular chaperones responses were represented as percentages in diverse brain regions and were measured against the WP-control group (Fig. 6).

Overall, the heat map of gene expression measurements of the molecular chaperones indicated that the ER responses to sleep deprivation stressor appears to be region specific, as indicated by the strong up-regulation of the majority of the ER chaperones genes in cerebellum, thalamus, parietal and brainstem. Although to a lesser level, the hippocampus also displayed up-regulation of ER chaperones genes compared to WP-control (Fig. 6). It should be noted that the stronger ER gene up-regulation response was following 48 h of sleep deprivation (SD-48 h), followed by the SD-72 h time point for all the brain regions with the exception of the frontal lobe. The frontal lobe showed the majority of ER up-regulation at 96 h of sleep deprivation (SD-96).

	Differential Modulation ER Chaperones Genes									
Region	Group	CANX	CALR	HSP90AB1	HSP90B1	HSPA2	HSPA4	HSPA5	HSPB1	PDIA4
Frontal	SD-48h	-13.70%	-20.54%	-21.77%	-20.72%	-18.63%	-21.13%	-7.53%	17.24%	-4.35%
	SD-72	-0.17%	-20.45%	-27.59%	-20.45%	-6.97%	-15.57%	9.05%	-15.56%	-3.68%
	SD-96	42.65%	22.41%	8.49%	5.82%	18.30%	8.49%	30.74%	-8.07%	11.28%
	HC-Control	14.27%	-10.19%	-7.07%	-9.98%	-9.61%	-5.67%	-6.26%	-20.75%	0.06%
	WP-Control	0.00%	0.00%	0.00%	0.00%	0.00%	0.00%	0.00%	0.00%	0.00%
Cerebellum	SD-48h	101.74%	38.83%	35.50%	48.54%	-26.41%	80.98%	77.87%	37.63%	44.73%
	SD-72	159.22%	34.10%	45.23%	57.73%	-13.80%	125.92%	117.47%	28.64%	52.98%
	SD-96	60.68%	14.27%	47.43%	37.47%	-17.88%	87.58%	36.05%	11.37%	32.56%
	HC-Control	-15.28%	-6.91%	-4.18%	-7.07%	3.47%	-8.99%	-16.73%	-23.11%	-14.83%
	WP-Control	0.00%	0.00%	0.00%	0.00%	0.00%	0.00%	0.00%	0.00%	0.00%
Hippocampus	SD-48h	19.82%	19.68%	28.05%	52.36%	-24.74%	17.01%	-20.83%	14.04%	95.09%
	SD-72	-6.32%	3.11%	17.28%	19.96%	-23.42%	-4.29%	15.27%	-17.41%	48.88%
	SD-96	-27.93%	-14.69%	-16.10%	1.69%	-13.85%	-24.91%	1.05%	-30.09%	12.62%
	HC-Control	-5.99%	-3.57%	-1.49%	9.62%	11.86%	-13.85%	10.83%	16.03%	18.71%
	WP-Control	0.00%	0.00%	0.00%	0.00%	0.00%	0.00%	0.00%	0.00%	0.00%
Parietal	SD-48h	-5.50%	35.90%	15.14%	25.85%	-12.69%	20.23%	-14.47%	2.74%	11.09%
	SD-72	-19.89%	18.85%	5.09%	13.16%	-0.75%	10.38%	9.24%	-5.39%	3.89%
	SD-96	-7.56%	8.61%	10.57%	3.41%	-2.34%	13.48%	11.00%	-14.30%	4.73%
	HC-Control	-25.00%	7.12%	14.39%	2.46%	-8.25%	14.14%	-15.88%	-25.31%	-22.44%
	WP-Control	0.00%	0.00%	0.00%	0.00%	0.00%	0.00%	0.00%	0.00%	0.00%
Thalamus	SD-48h	25.12%	21.14%	23.26%	34.10%	11.21%	14.08%	50.70%	-17.68%	11.60%
	SD-72	-9.35%	1.05%	1.51%	7.55%	-13.45%	-15.42%	-6.80%	-26.87%	-11.73%
	SD-96	-0.35%	27.31%	13.81%	27.02%	-4.18%	3.65%	39.80%	-25.46%	17.96%
	HC-Control	14.60%	10.57%	5.82%	8.30%	-7.56%	7.80%	30.13%	-24.53%	11.47%
	WP-Control	0.00%	0.00%	0.00%	0.00%	0.00%	0.00%	0.00%	0.00%	0.00%
Brain Stem	SD-48h	12.51%	40.69%	29.46%	49.48%	24.04%	12.25%	62.45%	25.48%	16.41%
	SD-72	8.55%	40.85%	18.44%	45.06%	35.27%	13.81%	61.33%	6.14%	9.11%
	SD-96	-2.40%	1.57%	-11.88%	7.18%	3.35%	-2.17%	13.94%	-5.94%	-2.45%
	HC-Control	-4.63%	3.23%	-12.59%	-4.96%	-12.39%	-5.18%	7.80%	-20.86%	-13.80%
	WP-Control	0.00%	0.00%	0.00%	0.00%	0.00%	0.00%	0.00%	0.00%	0.00%

Up
>300%
201 - 300%
101 - 200%
51 - 100%
25 - 50%
<25%
No Change
<25%
25 - 50%
51 - 100%
101 - 200%
201 - 300%
>300%
Down

Figure 6. Differential modulation of ER molecular chaperones genes. The numbers and colors reflect the gene expression changes (up or down regulation) in percentage compared to mRNA amounts determined from animals exposed to the wide platform control conditions.

3.1.9. Serum metabonomics analysis using Nuclear Magnetic Resonance (NMR)

Blood metabolomics was investigated to assess metabolite changes (metabolite profiles) that could potentially lead to the identification of novel biomarkers indicative of sleep-deprivation-induced stress. NMR-based metabonomics analysis was performed on blood serum obtained from control and sleep-deprived animals. PCA analysis of the NMR data is the first step in determining whether differences in major metabolites exist between control and treatment groups. If PCA ellipsoids (± 2 SE) of the various treatment groups were found to overlap with the control group, or any other treatment group, than no significant difference between those groups would be expected. Therefore, no further analysis (supervised) would be required. Results from this investigation using an unsupervised PCA analysis is indicated in Figure 7.

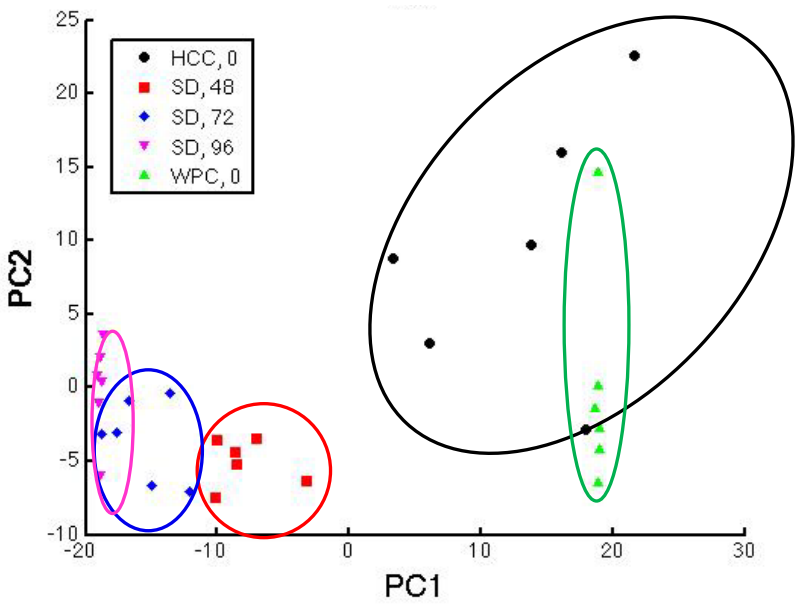

Figure 7. PCA scores plots (PC 1 vs. PC2) modeling the water platform control (WPC) and 96 h sleep-deprived rats (SD96). Here all groups have been superimposed into the model. The plots show individual subjects belonging to each group and the centroid mean ±2SE for each group. SD rats are identified at the 48 h (red), 72 h (blue), and 96 h (magenta) time points. The control animals are identified as home caged controls (HCC; black) and water platform controls (WPC; green). Data were auto-scaled to SD96.

The PCA plot in Figure 7 clearly shows that all SD animals from 48 to 96 h of sleep deprivation clearly separate from the control animals. While the PCA ellipsoids of the 48 h and 96 h SD animals clearly separate from each other, that of the 72 h SD animals overlapped with both of the other time points. This result was more than likely due to the larger variability in the data from the 72 h SD group. However, the PCA analysis shows that there are differences between the control and SD animals. In addition, it was observed that there was no difference between the two control groups (HCC and WPC). The results from the PCA analysis of the NMR data indicate that further supervised analysis is needed to identify those features that were responsible for this class separation.

We explored the ability to classify experimental groups using OPLS-DA. Initial OPLS-DA indicated that control rats can be classified separately from SD rats with high confidence (data not shown). When the analysis was limited to only the WPC group vs. SD rats at 96 h (data not shown), the Q^2 value was found to be 0.831 and the predictive accuracy was 92% (leave-one-out cross validation). The highest classification power was achieved in an OPLS-DA modeling of all controls vs. the SD rats at 96 h. The T-score plot shown in Figure 8 is from this analysis depicts these two groups along with the SD-48 h rats superimposed into the model. The Q^2 value was found to be 0.913 and the predictive accuracy was 100%. Here, the two control groups overlap, but the SD rats are clearly separated from controls and from each other at 48 h and 96 h. Interestingly, the number

of significant variables (loadings) is quite high as the analysis yields 52 highly significant features (bins) with alpha set at 0.001 (Table 10). The scope of this project did not include a full analysis of the spectral features that help to discern these experimental groups, as the timeframe (2 months) did not allow such an extensive analysis. However, significant bins are shown in Table 10. Further analyses would be necessary to probe these spectral regions to identify which metabolite signals are present and to determine how they may differ between experimental groups.

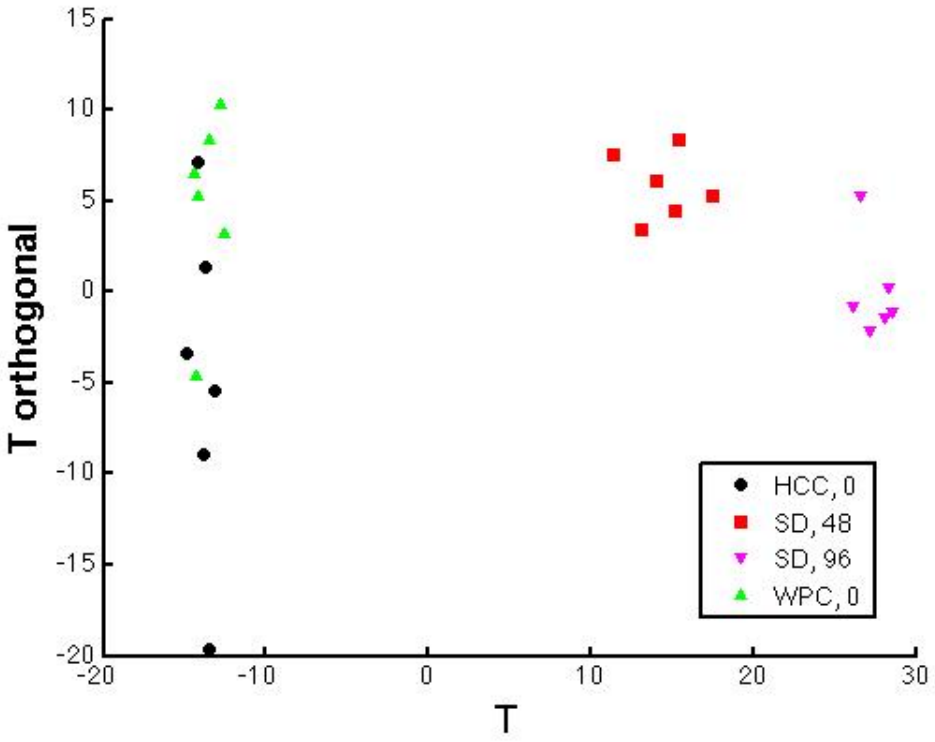

Figure 8. OPLS-DA model for all control rats (black) vs. SD rats at 96 h (filled red circles). All controls were entered into the model as a single group, but HCC (open squares) and WPC (filled squares) rats are identified separately in the plot. The SD rats at 48 h (open red circles) have been superimposed into the model and are separated from the 96 h SD rats. The model is highly significant yielding a Q^2 value of 0.913 and predictive accuracy of 100%. All data were auto-scaled to the SD group (all time points).

Table 10. List of significant bins (spectral features), in rank order, derived from the OPLS-DA shown in Figure 8. The chemical shift value (o) defines the position of the bin center (in ppm). These significant variables were determined using a permutation method involving 1,000 permutations with alpha set at 0.001.

Rank	6 (ppm)	Rank	6 (ppm)
1	2.271	27	1.665
2	4.306	28	5.633
3	1.316	29	3.965
4	2.261	30	1.112
5	1.611	31	1.688
6	2.291	32	3.749
7	2.276	33	3.499
8	5.238	34	3.512
9	5.346	35	2.538
10	2.864	36	3.888
11	1.407	37	2.437
12	4.323	38	3.450
13	2.049	39	4.191
14	2.241	40	3.071
15	1.176	41	1.733
16	4.098	42	4.430
17	5.215	43	1.099
18	0.878	44	3.434
19	3.542	45	2.390
20	2.111	46	3.642
21	2.834	47	5.425
22	1.432	48	7.875
23	5.269	49	1.031
24	4.293	50	3.244
25	3.278	51	7.403
26	3.925	52	1.084

3.2.0. Results Phase II: Effects of ADNP-8 and CNTF-11 peptide treatments against 96h sleep deprivation

Phase II of this study involved three weeks pre-treatment before the animals were exposed to sleep deprivation environment and four days treatment during sleep deprivation. For this study, animals were intranasal pre-treated/treated with 15 µg/kg of activity dependent neuroprotective protein-8 (ADNP-8), 750 µg/kg of ciliary neurotrophic factor 11 (CNTF-11) and a mix of ADNP-8 and CNTF-11 of the same dose as the single peptides. We also included control group that were dosed with a none-specific sequence

AA's (control AA's; see Table 3). Diverse biochemical, molecular and histological evaluations were performed. Results of these analysis are shown below.

3.2.1. Peptide treatment and weight gain/loss. Animals were weighed before and after 96 h of sleep deprivation. Results of this investigation demonstrated that peptide treatment did not prevent sleep deprivation-induced weight loss (Fig 9).

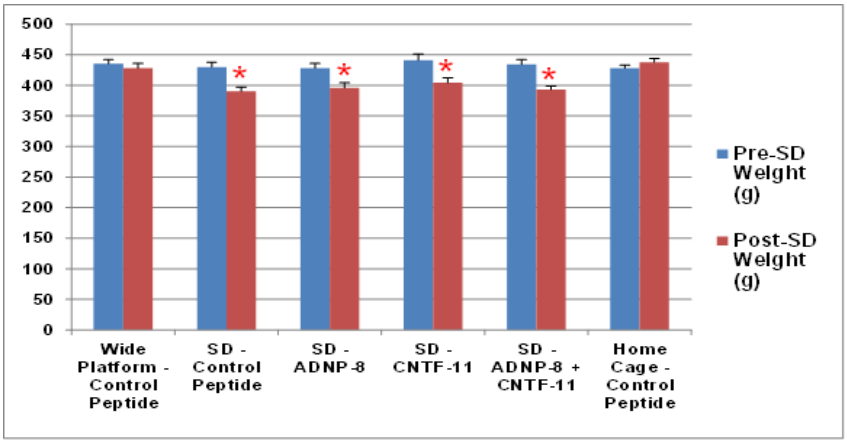

Figure 9. Effects of peptide treatment in weight loss after 96 h sleep deprivation. Peptide treatment did not prevent the weight loss in sleep deprived animals. *Represent statistical difference ($p \leq 0.05$) compared to pre-SD weight.

3.2.2. Effects of peptide treatment in blood corticosterone measurements

We measured serum corticosterone levels after 96 h sleep deprivation. Results indicated a significant difference ($p \leq 0.05$) in corticosterone levels from home cage control peptide and wide platform control peptide compared to the SD control peptide. A positive trend ($p \leq 0.1$) of sleep deprivation (SD) group treated with ADNP-8 was also observed when compared to the SD control peptide (Fig. 10).

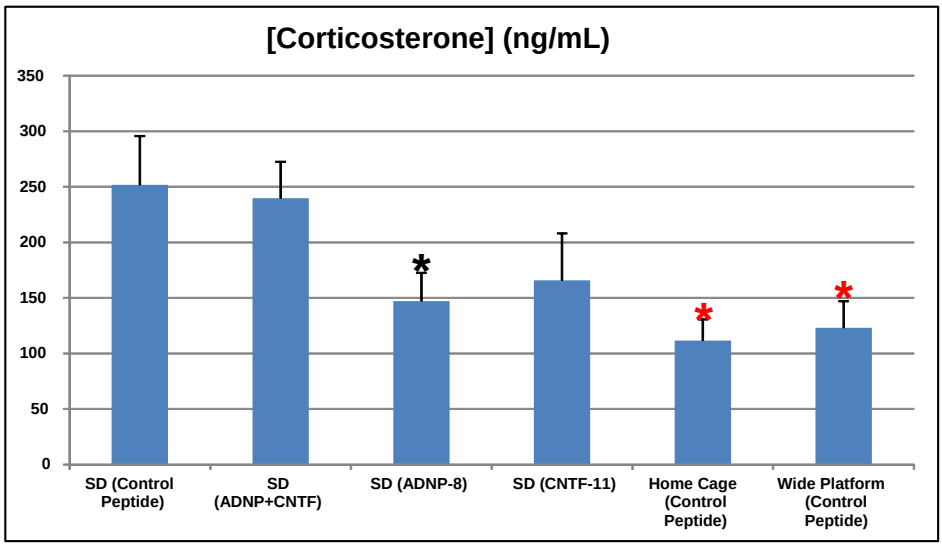

Figure 10. Representation of blood serum corticosterone concentration.*Corticosterone levels are significantly ($p \leq 0.05$) reduced in home cage and wide platform control compared to SD control peptide as indicated by red star. *A decrease was also observed in the SD (ADNP-8) group but did not reach a significance level ($p \leq 0.1$) at these experimental numbers.

3.2.3. Effects of peptide treatment in Protein oxidation

Generally, the peptide treatment did not show a significant difference in protein oxidation after 96 h sleep deprivation. With the exception of SD-(ADNP-8) frontal and Home Cage parietal groups showing a significant increase in protein carbonyl oxidation, no significant differences were observed in any other group (Table 11).

Table 11: Protein oxidation. Values representing the concentration of protein carbonyl in different brain sections. Numbers represent the average of six animals (n=6) ± standard deviation. ⁺Group dosed with control peptide; *significantly different ($p \leq 0.05$) compared to SD-control.

	Brain regions					
Groups	**Frontal (nmol)**	**Hippocampus (nmol)**	**Thalamus (nmol)**	**Cerebellum (nmol)**	**Parietal (nmol)**	**Brainstem (nmol)**
⁺SD	1.46±0.18	1.42±0.15	1.73±0.31	1.36±0.05	1.43±0.12	1.75±0.26
SD (ADNP+CNTF)	1.56±0.06	1.34±0.03	1.43± 0.08	1.81±0.41	1.32±0.02	1.66±0.14
SD (ADNP-8)	*1.76±0.14	1.40±0.08	1.58±0.26	1.57±0.33	1.39±0.05	1.75±0.23
SD (CNTF-11)	1.52±0.27	1.53±0.29	2.06±0.29	1.59±0.15	1.36±0.04	1.86±0.14
⁺Home Cage	1.70±0.39	1.46±0.17	1.52±0.09	1.41±0.11	*1.87± 0.36	2.26 ± 0.52
⁺Wide Platform	1.60±0.25	1.40±0.06	1.89±0.35	1.67±0.11	1.38±0.04	2.11 ± 0.54

3.2.4. Effects of peptide treatment in Lipid peroxidation

Lipid peroxidation represents the oxidative degradation of lipids in which free radicals (hydroxyl radical, superoxide anion, hydroxyl anion, and oxide anion) remove electrons from lipids in cell membrane causing cell damage or oxidative stress. The end products of lipid peroxidation are reactive aldehydes including malondialdehyde (MDA). In this study, we used a TBARS assay that reacts with MDA to yield a measurable fluorescent product that allows the quantitation of lipid peroxidation in selected brain regions. None of the testing groups showed a significant difference when compared with the SD control group. However, the home cage control group displayed a MDA value significantly higher ($p \leq 0.01$) in the hippocampal brain region when compared to SD group (Table 12).

Table 12. Lipid peroxidation measured in diverse brain regions. Values represent the averages ± standard deviation of MDA (µM) of six animals (n=6) group. ⁺Group dosed with control peptide; *significantly different ($p \leq 0.01$) compared to SD control.

	Brain regions					
Groups	**Frontal MDA(µM)**	**Hippocampus MDA(µM)**	**Thalamus MDA(µM)**	**Cerebellum MDA(µM)**	**Parietal MDA(µM)**	**Brainstem MDA(µM)**
⁺SD	25±4	19±3	22±6	21±4	28±6	10±3
SD (ADNP+CNTF)	28±3	21±4	20±3	20±3	27±3	11±2
SD (ADNP-8)	30±8	23±3	16±5	26±10	22±3	12±3
SD (CNTF-11)	35±12	26±8	18±3	21±4	24±4	13±2
⁺Home Cage	24±6	*29±6	19±4	20±4	24±3	13±4
⁺Wide Platform	24±5	21±4	17±2	21±4	26±4	12±3

3.2.5. Effects of peptide treatment in glutathione peroxidase activity

In this study, a significant increase in GPx activity was observed in the frontal cortex of groups including SD-(ADNP-8), SD-(CNTF-11), home cage and wide platform compared to SD-control group; suggesting an enhanced protection of the individual peptides treatment against oxidative stress. Unexpectedly, a significant decrease in GPx activity was also observed in thalamus (wide platform) and cerebellum SD-(CNTF-11) (Table 13).

Table 13. Representation of the effects of peptide treatment GPx activity (nmol/min/mL) in different brain regions. ⁺Group dosed with control peptide; *significantly different ($p \leq 0.05$) compared to SD control.

	Brain regions					
Groups	Frontal Gpx	Hippocampus Gpx	Thalamus GPx	Cerebellum Gpx	Parietal Gpx	Brainstem Gpx
+SD	58±13	71±6	120±9	120±16	97±13	109±19
SD (ADNP+CNTF)	*91±37	85±34	130±23	111±21	87±19	106±20
SD (ADNP-8)	*98±31	66±7	123.8±21	113±18	90±15	107±5
SD (CNTF-11)	*92±11	64±6	110±29	*94.7±7	96±19	92±4
+Home Cage	*91±11	69±15	118±35	120±20	97±29	105±19
+Wide Platform	*87±10	68±8	*94±10	131±27	86±21	100±13

3.2.6. Effects of neuropeptide treatment in superoxide dismutase (SOD) activity

SOD is a very important defense to protect the cell against oxidative stress. Results of these measurements indicated no significant different in SOD activity in almost all the testing groups and brain regions compared to SD-control group (table 13). Surprisingly, a significant ($p \leq 0.001$) increase of SOD activity in cerebellum for the HC-control was observed. In addition, HC-control group also displayed a significant ($p \leq 0.001$) decrease in SOD activity in brainstem. The reason for the increase/decrease in these two brain regions for this experimental group is unknown.

Table 14. Effects of peptide treatment in SOD activity in diverse brain regions. ***Indicates a significant increase compared to SD-control. *****Indicates a significant decrease compared to SD-control. +Group dosed with control peptide.

	Brain Regions					
Group	Frontal (U/min/ml)	Cerebellum (U/min/ml)	Hippocampus (U/min/ml)	Parietal (U/min/ml)	Thalamus (U/min/ml)	Brainstem (U/min/ml)
+SD-Control	11±10	8±8	55±11	78±27	66±13	31±2
SD-(ADNP-8 + CNTF-11)	20±15	15±11	46±13	84±12	51±12	35±11
SD-ADNP-8	12±17	15±14	53±5	75±12	61±31	30±7
SD-CNTF-11	15±15	14±15	47±9	68±13	78±50	33±9
+Home Cage	9±10	*36±8	56±19	63±10	81±47	*8±11
+Wide Platform	10±10	17±14	62±19	62±12	64±22	33±12

3.2.7. Effects of neuropeptide treatment against neuronal cell death

As previous investigations have shown the role of small peptide ADNP-8 in protecting neuronal cells against damage and aiding recovery after traumatic brain injury. In

addition, the CNTF-11 has been investigated as a potential peptide to stimulate neurogenesis. In this study, we used brain tissue from prefrontal cortex, hippocampus and thalamus to perform immunohistochemistry analysis including: 1) Fluoro-Jade B staining to measure neuronal cell death, 2) TUNEL assay to evaluate apoptotic cell death and 3) Doublecortin (DCX) as a protein to measure new neuron formation. For each of the brain regions, a total of three brain tissue coronal sections 10 µm thick were cut using a freezing sliding microtome. Tissue was examined using a confocal microscope with excitation light at 515 nm. The number of dead cells, apoptotic or new cells formation were assessed from ten 10X microscope fields. Different areas of each slice were taken for a total of 30 fields/brain region/animal (n=6). For each animal, the total number of cells was averaged across the fields resulting in average # of neurons/field of view. These averages were used for statistical analysis using student t-test with a $p \leq 0.05$. The use of these techniques allowed us to investigate the effectiveness of ADNP-8 and CNTF-11 in protecting the brain from cellular death caused by acute sleep deprivation.

3.2.8. Neuronal cell death assessment of frontal cortex

The frontal cortex is considered a very important part of the brain and extremely sensitive to external and internal stimuli. The frontal cortex in humans, plays an important role in cognitive processes called executive functions that include working memory, reasoning, planning and problem solving. In this study, we used a Fluoro-Jade B staining method that uses a fluorochrome to label degenerating neurons in tissue sections from perfused brain. A total of three samples of brain tissue coronal sections 10µm thick from the anterior, middle and posterior section of the frontal cortex were cut using a freezing sliding microtome. Fluoro-Jade positive neurons were subsequently counted from each field using *Image J software.* Unexpectedly, with the exception of the SD-(ADNP-8+CNTF-11) group, the number of neuronal cell death was significantly increased in all the experimental groups compared to the SD-control (Fig. 11). This result could be that the frontal lobe is highly sensitive to sleep deprivation, and after 96 h of sleep deprivation an abundant number of necrotic neurons have been already reabsorbed at earlier time points by the microglia resulting in low neuronal cell death staining for the SD-control group.

In addition, TUNEL assay was also used to investigate apoptotic cell death. Consistent with the Fluoro-Jade results, a significant increase in apoptotic cells was observed in SD-(ADNP-8+CNTF-11), SD-ADNP-8 and WP-control yielding values of 44 ± 4, 44 ± 5 and 49 ± 6, respectively, compared to SD-control (38 ± 2). Furthermore, a decrease was observed in SD-CNTF-11 and HC-control, however, only HC-control reached a statistical significance $p \leq 0.04$ (Fig. 12). The reason for the unexpected increase in apoptotic cell death, including the controls, remains unknown.

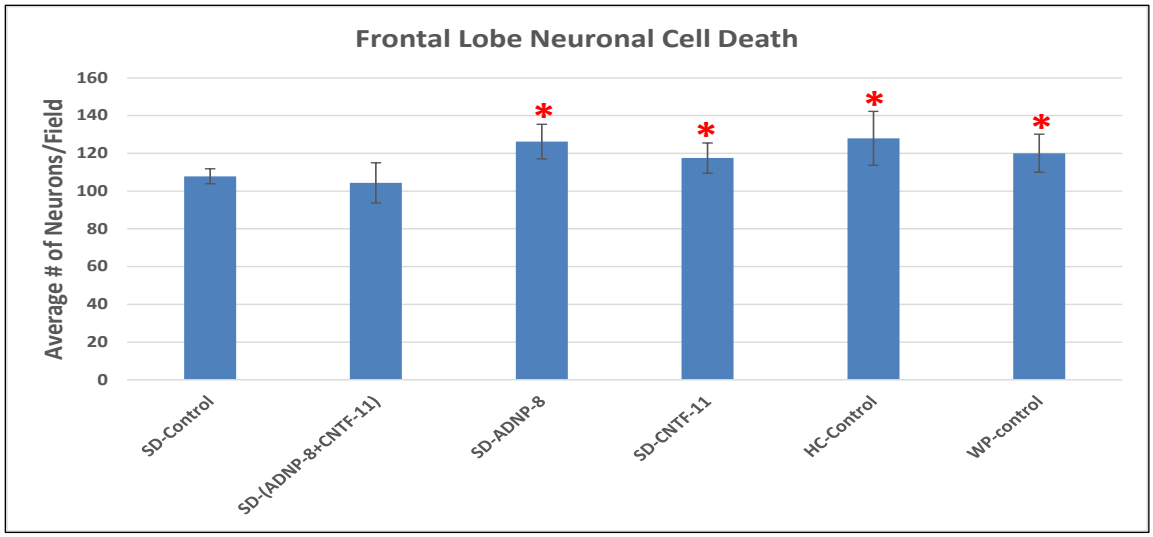

Figure 11. Graphical representation of neuronal cell death in frontal lobe after 96 h sleep deprivation. *Represents significant p ≤ 0.05 increase compared to SD-control group.

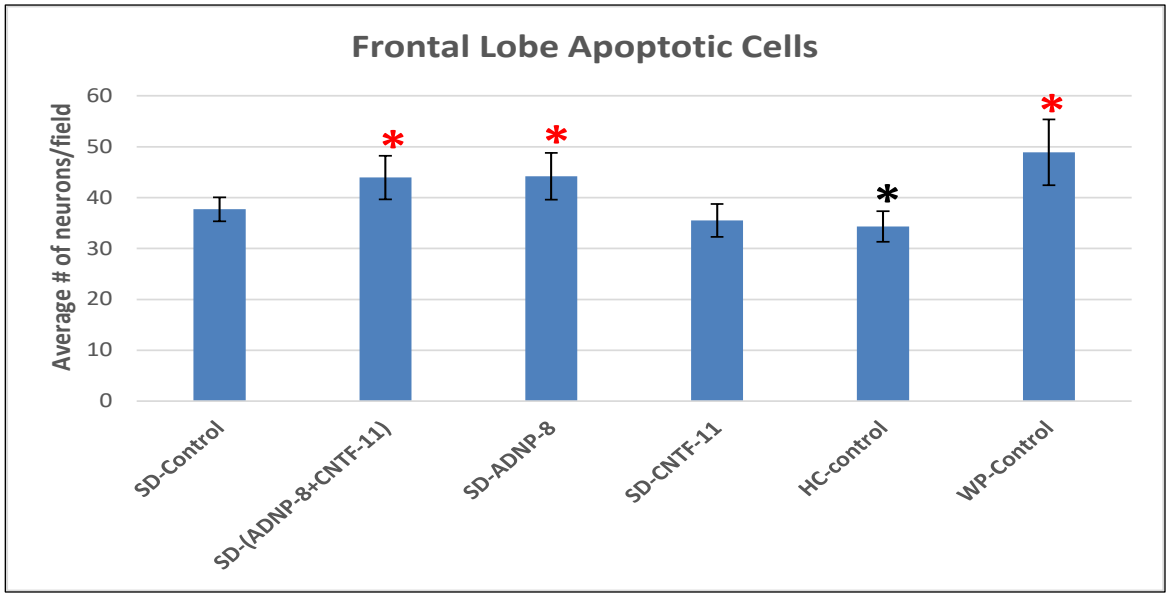

Figure 12. Graph illustrating apoptotic cells after 96 h sleep deprivation. *Indicates a significant (p ≤ 0.05) increase. *A significant decrease p ≤ 0.04 compared to SD-control group.

3.2.9. Neuronal cell death assessment of hippocampus

The hippocampus is an important component of the brain playing a key role in the formation and consolidation of information from short term memory to long term memory and spatial navigation. The hippocampus is highly vulnerable to stress causing a

decrease in neurogenesis in the dentate gyrus, atrophy in dendrites growth and eventually neuronal cell death. The effectiveness of the neuropeptide treatments against 96 h of sleep deprivation was measured by the number of dead neurons in hippocampus and dentate gyrus of this brain region detected by Fluoro-Jade staining. Results of this investigation indicated a significant reduction ($p \leq 0.01$) in neuronal cell death for SD-ADNP-8 and SD-(CNTF-11 + ADNP-8) groups yielding values of 67 ± 4 and 57 ± 4, respectively, when compared to the SD-control group (72 ± 3). Expectedly, the HC-control peptide and WP- control peptide also yielded significant ($p \leq 0.01$) reduction in neuronal death; 62 ± 2 and 60 ± 6, respectively, compared to SD-control peptide group (Fig. 13).

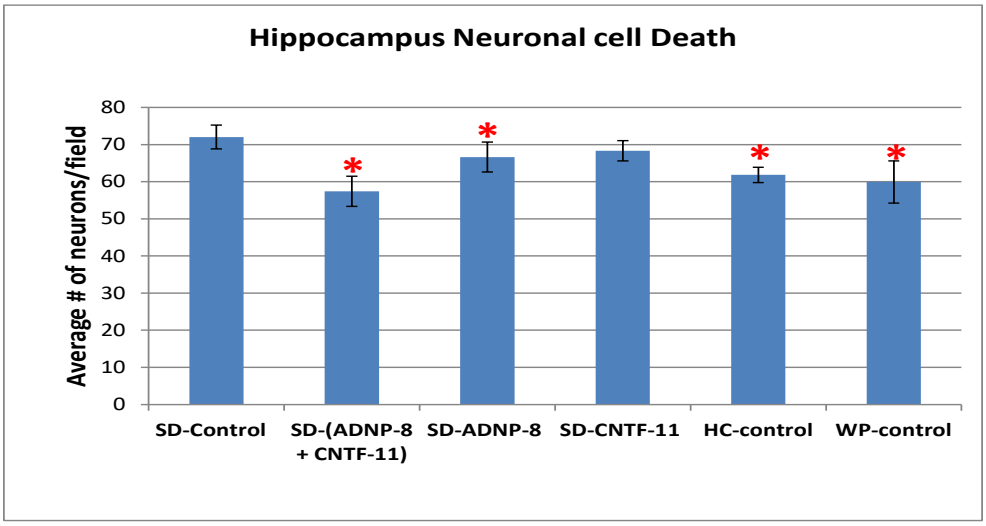

Figure 13. Representation of neuronal cell death in hippocampus detected by Fluoro-Jade staining. *A significance ($p \leq 0.01$) reduction of neuronal cell death was observed in the groups represented in the bargraph.

Additionally, the neuronal cell death was also measured in the dentate gyrus of the hippocampus (Fig. 14). Results showed a significant reduction ($p \leq 0.01$) for the SD-(ADNP-8 + CNFT-11) peptide treatment yielding a value of 108 ± 5 compared to the SD-control (115 ± 20); this suggests the effectiveness of the combination of these peptides in preventing neuronal cell death. As expected, the WP control peptide also displayed a significant ($p \leq 0.01$) reduction (101 ± 8) in neuronal cell death compared to SD-control peptide group. Therefore, we can suggest that the mixture of ADNP-8 + CNTF-11 is the more effective treatment to prevent neuronal cell death in hippocampus and dentate gyrus after 96 h sleep deprivation (Fig. 13 and 14). Unexpectedly, the HC-control and SD-CNTF-11 showed a significant ($p \leq 0.01$) increase of 130 ± 4 in neuronal cell death compared to SD-control (Fig 14). As mentioned above, this finding could be that the number of dead neurons for the SD-control at this time point have already been reabsorbed resulting in less neuron cell death detection when using Fluoro-Jade staining.

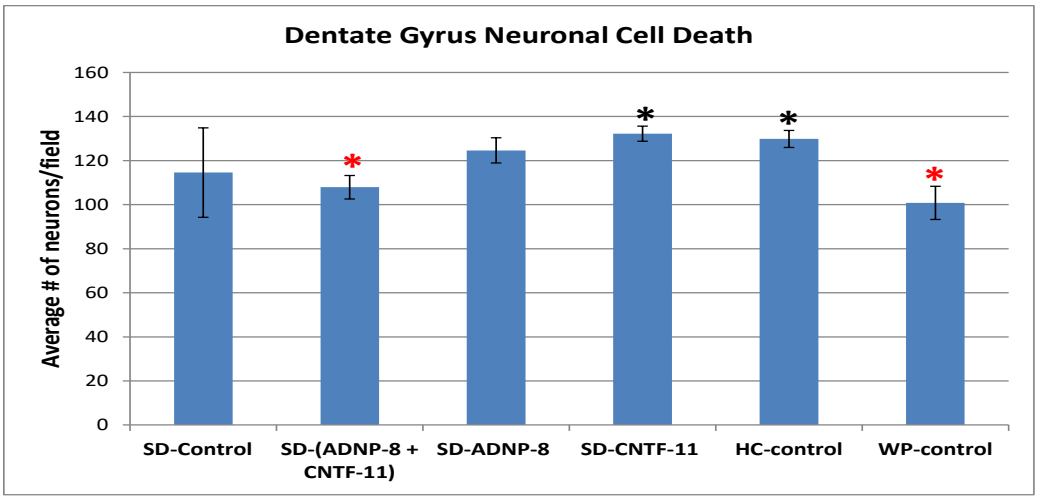

Figure 14. Neuronal cell death in the dentate gyrus of hippocampus. *A significant reduction ($p \leq 0.01$) in neuronal cell death was observed. Surprisingly, *SD-CNTF-11 and HC-control displayed a significant increase in cell death compared to SD-control.

Furthermore, TUNEL assay was also completed in hippocampus to assess the effectiveness of the peptide treatments against apoptotic cell death. Results indicated no significant effect of any of the peptide treatments in preventing apoptotic cell death (Fig. 15). As expected, the WP-control displayed a significant ($p \leq 0.0002$) reduction in apoptotic cells compared to SD-control with values of 34 ± 2 and 39 ± 3, respectively.

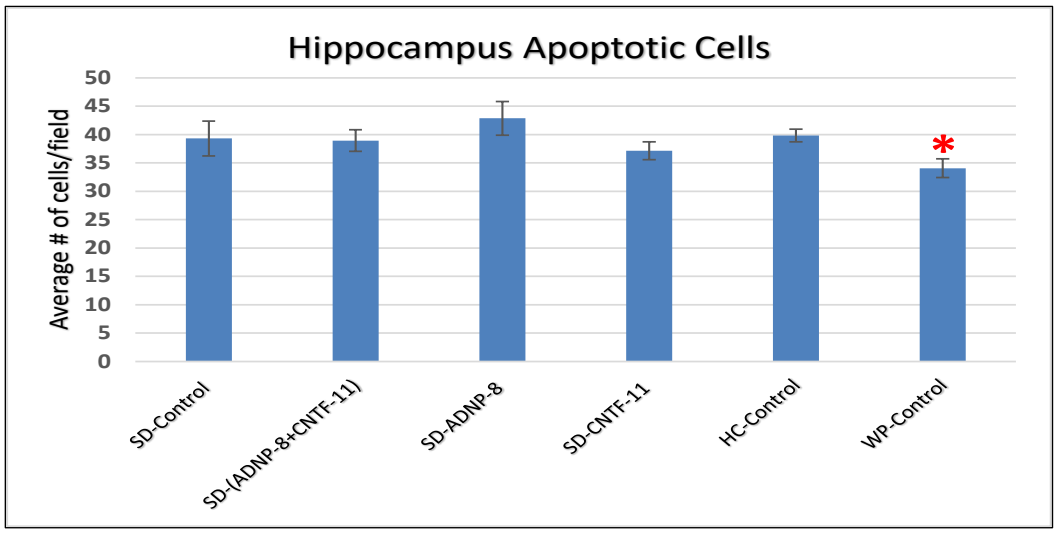

Figure 15. Graph representing apoptotic cells detected by TUNEL assay.

In addition, apoptotic cell death was also assessed in the dentate gyrus of hippocampus. Results of this investigation indicated no significant differences in any of the experimental treatment groups compared to SD-control group (Fig. 16).

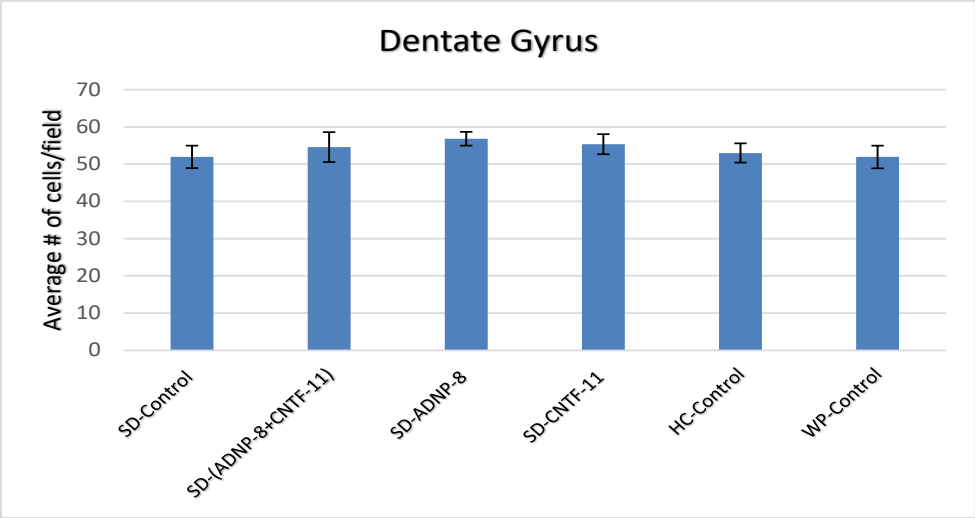

Figure 16. Representation of apoptotic cell death in dentate gyrus after 96 h sleep deprivation.

3.2.10. Neuronal cell death assessment in thalamus

The thalamus is a brain structure situated between the cerebral cortex and the midbrain. This brain structure functions as a relay between the different sub-cortical areas and the cerebral cortex. Some of the thalamus functions include sensory and motor signals to the cerebral cortex. In addition, the thalamus is also involved in regulation of consciousness, sleep and alertness. The number of neuronal cell death and apoptotic cells was measured using Fluoro-Jade staining and TUNEL, respectively. Results indicated that the peptide treatments were not effective in reducing neuronal cell death in this brain region. Unexpectedly, the number of dead neurons were significantly elevated in all the experimental treatment groups compared to SD-control (Fig. 17). Conversely, analysis of the number of apoptotic neurons was significantly ($p \leq 0.01$) reduced in SD-(ADNP-8+CNTF-11) group (37 ± 5) compared to SD-control (43 ± 4). Expectedly, the number of dead neurons was also reduced in WP-control peptide (39 ± 3). Unpredictably, an increase in the number of apoptotic and dead neurons was also observed in the SD-HC control peptide (Fig. 18).

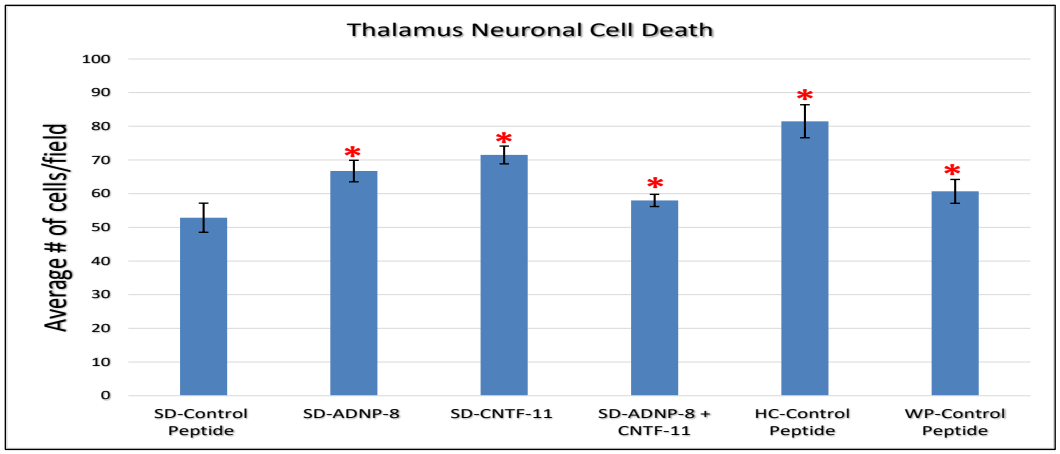

Figure 17. Illustration of the neuronal cell death in thalamus. *Represent statistical significance ($p \leq 0.01$) compared to SD-control group.

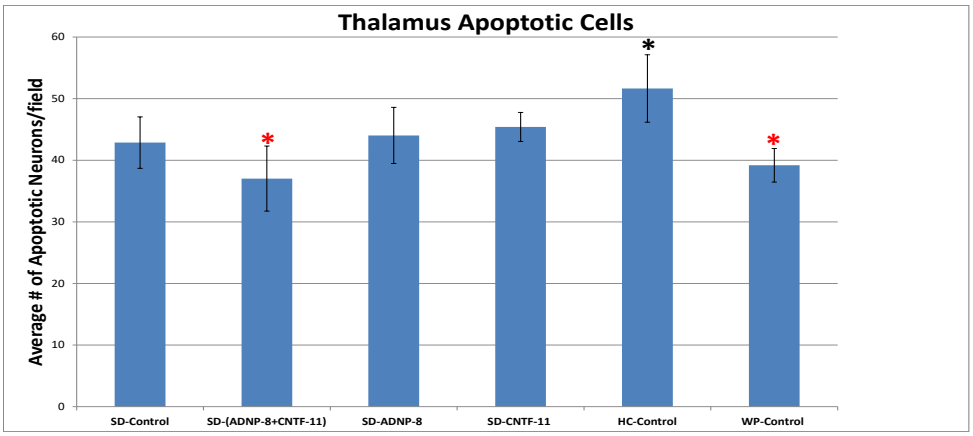

Figure 18. Number of apoptotic cells in the thalamus. *A significant reduction ($p \leq 0.01$) in the number of neuronal cell death was observed. *HC-control displayed a significant ($p \leq 0.01$) increase in cell death compared to SD-control.

3.2.11. Effectiveness of peptide treatments in hippocampal neurogenesis

Doublecortin (DCX) is a microtubule-associated protein expressed by neuronal precursor cells and immature neurons in embryonic and adult cortical structures. Neuronal precursor cells begin to express DCX while actively dividing, and their neuronal daughter cells continue to express DCX for 2–3 weeks as the cells mature into neurons. Once neurons reach four weeks old, expression of DCX down-regulates dramatically and these neurons begin to express Neuronal Nuclear protein (NeuN), which is a marker for detecting mature neurons. In this study, we used DCX to evaluate the effects that acute sleep deprivation has on the formation of new neurons (neurogenesis) in the dentate gyrus of the hippocampus. In addition, the effect of treatments with small peptides

(ADNP-8 and CNTF-11) in the formation of new neurons was also evaluated. Results of this investigation indicated a significant increase ($p \leq 0.01$) in the formation of new neurons for all experimental treatment groups, including SD-CNTF-11, SD-ADNP-8, SD-(ADNP-8 + CNTF-11), HC-control and WP-control groups yielding values of 23 ± 4, 18 ± 1, 19 ± 2, 26 ± 2 and 33 ± 5, respectively, compared to SD-control (17 ± 1). CNTF-11 peptide treatment showed the highest benefits in stimulating neuronal cell proliferation with a value of 23 ± 4. As expected, the WP-control (less stressed group) showed the greatest number (33 ± 5) of new neurons (Fig. 19).

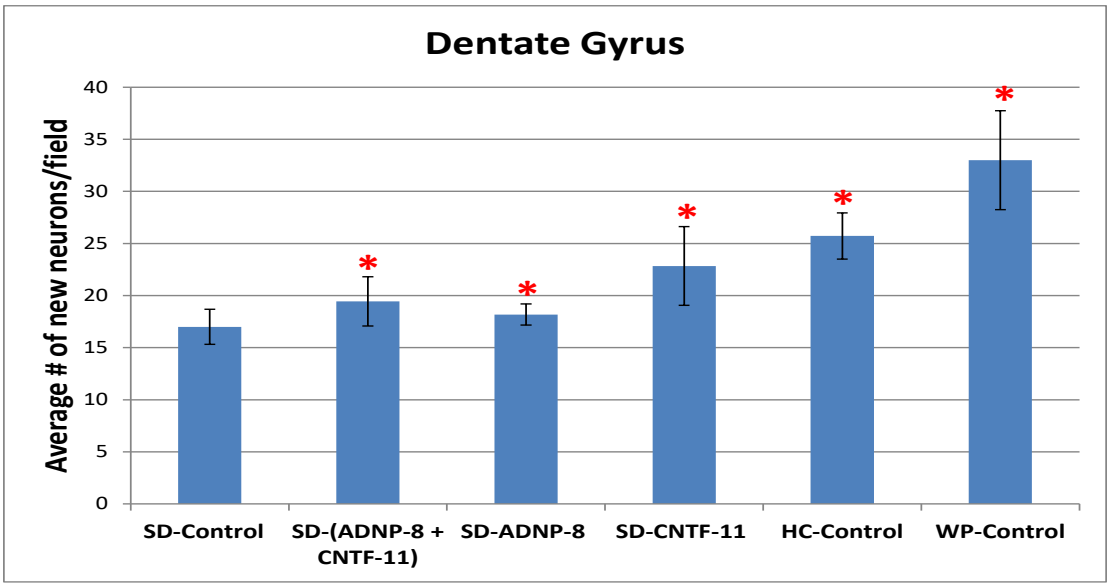

Figure 19. Number of new immature neurons detected in dentate gyrus of hippocampus. *Indicates a significant difference compared to SD-control group.

3.2.12. Effects of neuropeptide treatment in unfolded protein response

The gene expression profiles of molecular chaperones CANX, CALR, HSP90AB1, HSP90B1, HSPA2, HSPA4, HSPA5, HSPB1 and PDIA4 were measured after 96 h of sleep deprivation. To evaluate the expression of these molecular chaperones, a heat map was created using the CT values of the peptide treatments and compared to the CT value of SD-control. The CT values were converted to % of expression taking as reference the % of the SD-control equal to 0% or no change (white color) and green and red color representing down- or up-regulation, respectively. In general, results from the heat map indicated a down-regulation of the molecular chaperones in almost all the brain regions and experimental groups compared to SD-control. In the cerebellum, an up-regulation of HSPA2 and HSPB1 molecular chaperones was observed in all the experimental groups. In the parietal lobe, ADNP-8 caused up-regulation of all the molecular chaperones. Overall, peptide treatments caused up-regulation of HSPB1 in all

brain regions. Taken together, the results of the heat map suggest that ADNP-8 was the most effective peptide treatment by stimulating various molecular chaperone responses; the cerebellum and parietal lobe and brainstem showed the most change responses to this peptide treatment (Fig. 20). In addition, ADNP-8 treatment caused stronger HSPB1 response in almost all brain regions. Another possibility is that the peptide treatment is protecting neurons through an unknown mechanisms helping cells to reach homeostasis and bring the ER molecular chaperones response to normal levels.

Brain Region	Group	ER Chaperone Genes								
		1	2	3	4	5	6	7	8	9
Frontal Lobe	A	0%	0%	0%	0%	0%	0%	0%	0%	0%
	B	-24%	-21%	-16%	-33%	-29%	-28%	-16%	6%	-13%
	C	-29%	-31%	-21%	-32%	-30%	-25%	-21%	7%	-19%
	D	-26%	-10%	-9%	-21%	-14%	-22%	-4%	13%	-13%
	E	-22%	-18%	9%	-10%	-18%	-2%	-16%	-32%	-6%
	F	-8%	-8%	-1%	-10%	-20%	-3%	-14%	-31%	-7%
Hippocampus	A	0%	0%	0%	0%	0%	0%	0%	0%	0%
	B	-9%	12%	7%	-18%	-25%	-25%	-18%	17%	-2%
	C	-6%	21%	-4%	-36%	-20%	-47%	-29%	14%	-21%
	D	-16%	-14%	-8%	-46%	-24%	-35%	-20%	-20%	-12%
	E	-16%	-16%	-31%	-40%	-22%	-47%	-56%	-25%	-40%
	F	-6%	-6%	-1%	-20%	-2%	-36%	-36%	-30%	-19%
Cerebellum	A	0%	0%	0%	0%	0%	0%	0%	0%	0%
	B	43%	32%	2%	6%	94%	26%	4%	147%	-13%
	C	-16%	30%	10%	2%	30%	4%	-6%	124%	-13%
	D	0%	-6%	-13%	-12%	70%	-14%	-18%	105%	-20%
	E	4%	-11%	-24%	-37%	63%	-30%	-42%	24%	-37%
	F	11%	4%	-33%	-48%	50%	-34%	-31%	18%	-29%
Parietal Lobe	A	0%	0%	0%	0%	0%	0%	0%	0%	0%
	B	40%	11%	22%	13%	34%	33%	36%	32%	28%
	C	7%	-7%	5%	-14%	0%	-24%	12%	25%	12%
	D	-38%	-31%	-27%	-32%	-27%	-37%	-27%	-24%	-21%
	E	6%	-18%	-18%	-22%	-4%	-18%	-33%	-27%	-31%
	F	15%	2%	-10%	-3%	14%	4%	-4%	-20%	2%
Thalamus	A	0%	0%	0%	0%	0%	0%	0%	0%	0%
	B	21%	-21%	-32%	-27%	-5%	-38%	-6%	-18%	-14%
	C	0%	-14%	-35%	-30%	-6%	-26%	-16%	3%	-3%
	D	-7%	13%	-14%	1%	37%	-21%	2%	27%	-10%
	E	-14%	-32%	-52%	-31%	3%	-16%	-36%	-53%	-26%
	F	-57%	-44%	-51%	-40%	-8%	-22%	-25%	-38%	-17%
Brainstem	A	0%	0%	0%	0%	0%	0%	0%	0%	0%
	B	-14%	-19%	-3%	-6%	-16%	-14%	-21%	86%	-29%
	C	-17%	-22%	-7%	-20%	-33%	-28%	-30%	27%	-21%
	D	-34%	-38%	-33%	-34%	-32%	-41%	-41%	10%	-26%
	E	-19%	-47%	-32%	-40%	-42%	-37%	-46%	-5%	-40%
	F	-21%	-44%	-31%	-36%	-38%	-46%	-41%	-11%	-32%

Experimental Group	
A	SD / Control Peptide
B	SD / ADNP-8
C	SD / CNTF-11
D	SD / ADNP-8 + CNTF-11
E	WP / Control Peptide
F	HC / Control Peptide

ER Chaperone Genes	
1	CANX
2	CALR
3	HSP90AB1
4	HSP90B1
5	HSPA2
6	HSPA4
7	HSPA5
8	HSPB1
9	PDIA4

Up-Regulation
>300%
201 - 300%
101 - 200%
51 - 100%
25 - 50%
<25%
No Change
<25%
25 - 50%
51 - 100%
101 - 200%
201 - 300%
>300%
Down-Regulation

Figure 20. Endoplasmic reticulum molecular chaperones response after 96 h sleep deprivation. Letters A-F represent the experimental groups and numbers 1-9 represent ER molecular chaperones genes (See key). The percentage measure of the ER genes providing up or down regulation are compared to A (SD-control group).

4.0 Discussion

4.1. Oxidative stress and antioxidant defense

Oxidative stress occurs when there is an imbalance between oxidant species production and antioxidant defense capabilities within the cell. Such imbalance in the cell causes oxidation of proteins, and lipids, DNA breakage and ultimately cell death. The brain may be particularly vulnerable to oxidative stress because of its high rate of oxygen consumption, high content of polyunsaturated fatty acids, and low levels of natural antioxidants defenses compared to other organs (18). In this study, we first investigated the effects of acute sleep deprivation on oxidative stress; this included oxidant production markers and the increase or decrease of antioxidant defense in different brain regions. In addition, tissue ER folding protein content during stress conditions was also measured by profiling a set of molecular chaperones' gene response. Second, we studied the efficiency of small peptides ADNP-8 and CNTF-11 against the adverse effects of sleep deprivation.

Lipid peroxidation occurs when free radicals react with lipids damaging the lipid bilayer of the cell membrane causing oxidative damage. In the present study, we observed an increased concentration of lipid peroxidation in the hippocampus after 48 and 72 h of sleep deprivation. Additionally, an increase in lipid peroxidation after 72 h was also observed in the parietal lobe. At 96 h of sleep deprivation, a significant reduction in lipid peroxidation was observed for the cerebellum, parietal and brainstem. Although a statistical difference was not reached, a trend in reduction of lipid peroxidation was also observed in the frontal lobe, hippocampus and thalamus at 96 h (Table 6). In addition, we also observed that the peptide treatments did not reduce the amount of protein oxidation in any of the brain regions after 96 h sleep deprived (Table 11). However, the low concentration of oxidative markers in the cell does not necessary exclude the presence of an oxidative stress during sleep deprivation. It is possible that the antioxidant defenses including GPx have already became activated before 96 h of sleep deprivation, reducing the levels of oxidative damage in the cell in a specific brain region. Low concentrations of oxidative markers of stress and antioxidant defense have been previously reported. For instance, Gopalakrishnan et al. reported no significant increase in lipid peroxidation, protein oxidation and superoxide dismutase (SOD) after 8 h to 14 days of sleep deprivation in cerebral cortex of rats (19). However, in this published study, the authors used only two animals (n=2) in each experimental group. Other studies have reported an increase of 8-isoprostane and MDA levels, which are lipid peroxidation markers, found in the serum as well as in the cortex, amygdala and the hippocampus after 24 h of sleep deprivation (20). It has been hypothesized that sleep loss affects different parts of the brain differently with regards to oxidative stress. Some studies have reported higher responsiveness of oxidative stress markers in hippocampus and hypothalamus, and reduced susceptibility to oxidative stress in cortex and brain stem in response to sleep deprivation (21 – 23). Conversely, others have reported increased oxidative stress in the hippocampus and cortex in sleep deprived rats (21 – 23). The discrepancies between studies may be due to different sleep deprivation models, or due to selection of different brain regions and time points. An important consideration

regarding the use of neuropeptides at 96 h of sleep deprivation is that, perhaps, using the peptide treatment a more likely span of time such as after 24 or 48 h of sleep deprivation will result in a better evaluation of the effectiveness of the peptides in preventing oxidative stress caused by lipid peroxidation.

Protein oxidation is an important factor in aging and age-related neurodegenerative disorders (34). Oxidative modification of proteins can lead to diminished specific protein functions, which may ultimately result in cell death (34). Protein oxidation is most often measured by the presence of protein carbonyls. Protein carbonyls arise from a direct free radical attack on vulnerable amino acid side chains, within the protein backbone or from the products of glycation, glycoxidation, and lipid peroxidation reactions with proteins (e.g., HNE and acrolein; 34). In our base line studies, we observed an increase in protein oxidation in parietal lobe and hippocampus after 48 h sleep deprivation (Table 7). In addition, at the 96 h time point, increased levels of protein oxidation were also observed in parietal and cerebellum, but not in thalamus or brainstem, suggesting that the susceptibly of different brain regions against sleep deprivation could be as a result of diverse levels of antioxidant defenses in each brain region. Diverse levels of protein oxidation in various brain regions have been reported in patients with Alzheimer's disease (35, 36). Also, in the same patients, different levels of antioxidant defenses have been found (37, 38). Conversely, in our peptide treatment experiments, no significant difference in protein oxidation was observed after 96 h sleep deprivation (Table 11). This result suggests that the peptide treatment was able to restore homeostasis and protected the cells from oxidative stress caused by acute sleep deprivation. However, the mechanistic action of the peptides against oxidative stress requires further investigation.

Free radicals can be difficult to accurately measure because of their rapid rates of formation and high reactivity with other cell components producing an overall cellular oxidative stress burden on normal homeostasis. However, the damage of free radical in cells is diminished by the production of antioxidant responses involving GPx and SOD. During the baseline study, GPx activity was increased in frontal, cerebellum, hippocampus and thalamus, but not in parietal lobe and brainstem during the first 48 h of sleep deprivation. In addition, GPx levels gradually decreased yielding the lowest level at 96 h of sleep deprivation (Table 8). This finding suggests that during the first hours of sleep deprivation, the cells' antioxidant defense capability is elevated in an attempt to prevent cell damage due to accumulation of free radicals. However, during the peptide treatment study, GPx activity increased only in frontal cortex and not in other brain regions; this might indicate that the protective activity for these neuropeptides is region specific (Table 13). The reason for the inconsistency in the increase or decrease in GPx activity in other brain regions or organs remains to be investigated. For instance, investigations have shown a 10% increase in GPx activity after 10 days of sleep deprivation in heart muscle, but not in liver (16). In addition, other investigations found decreased GPx activity in hippocampus and brainstem in sleep deprived rat for 5- 11 days (17). Further investigations revealed an increase in GPx activity in hippocampus and cerebellum, but not in hypothalamus, brain stem or basal forebrain after 6 h of total sleep

deprivation in rats (24). Taken together, these results suggest that the primary target of oxidative stress and/or antioxidant stress response may vary, depending on the cell type or brain region and/or the type and severity of stress.

The antioxidant defense systems consist of non-enzymatic molecules including glutathione as well as enzymatic scavengers such as SOD, catalase, and glutathione peroxidase. In the brain, where catalase and glutathione peroxidase activities are relatively low, the primary defense is represented by SOD (25 – 27). In our studies, we observed a significant decrease in SOD in the frontal lobe at 48, 72 and 96 h of sleep deprivation (Table 9). Hippocampus, parietal and brainstem also displayed a decrease in SOD after 96 h, while brainstem SOD levels decreased at 48 and 96 h of sleep deprivation. No differences were observed in cerebellum and thalamus. Additionally, no differences were observed during the peptide treatments after 96 h of sleep deprivation in all brain regions and all experimental groups, suggesting that the peptide treatment were unable to restore the activation of SOD at this time point (Table 14). Consistent with our results, other sleep deprivation studies have demonstrated a reduction in SOD activity in hippocampus and brainstem, but not in cerebral cortex, cerebellum and hypothalamus after 5-11 days of sleep deprivation (17); suggesting that different brain regions are more vulnerable than others to the effects of sleep deprivation. The possibility exist that after long period of sleep deprivation, the accumulation of reactive oxygen species is abundant causing a vast inhibition in SOD activity. It has been shown that under oxidative stress conditions, the overproduction of ROS is able to inhibit SOD activity (28).

4.2. Endoplasmic Reticulum Molecular Chaperones Response

All proteins, cytosolic and membrane, are folded and mature in the lumen of the endoplasmic reticulum (ER) before they are delivered to other compartments in the endomembrane system, displayed on the cell surface, or released extracellularly. The ER signal responds to a variety of signal transduction pathways to activate the unfolded protein response (UPR). The UPR monitor efficiency of protein folding in the ER. If a protein folding inefficiency occurs in the ER, the UPR response starts by activating mainly three sensor transducers: ATF6 (Activating Transcription Factor 6), PERK [PKR (RNA-dependent protein kinase)-like ER kinase] and IRE1 (Inositol Requiring Enzyme 1). Activation of each sensor transducer produces a transcription factor ATF6(N), XBP1, and ATF4, respectively, that activates molecular chaperone genes to increase the protein-folding capacity in the ER (29). Therefore, prolonged activity of the UPR can be an indication that ER stress cannot be alleviated and homeostasis cannot be reestablished. When protein production and folding homeostatic processes fail, the UPR can also serves as an activator of apoptotic genes. In our studies, we measured the ER molecular chaperones gene response against 48, 72, and 96 h sleep deprivation (Fig. 6). Generally, the heat map of the molecular chaperones expression indicated a stronger gene up-regulation for all the time points in cerebellum, followed by parietal lobe, thalamus, brainstem and hippocampus. In the frontal lobe, most of the gene up-regulation occurred after 96 h sleep deprivation. In addition, we also noticed that the strongest up-regulation

of all the genes studied occurred during 48 h and 72 h of sleep deprivation in all of the brain regions. At the 96 h time point, the earlier observed up-regulation was decreasing, reaching a negative values for some of the molecular chaperones genes and brain regions. This suggests that at this particular time point, the ER systems might be overwhelmed and the UPR is preparing to activate an apoptotic gene response. Furthermore, with exception of cerebellum, CANX, HSPA2 and HSPB1 displayed low up-regulation in all brain regions. Conversely, in our peptide treatment experiment, the heat map of the molecular chaperones expression indicated a down-regulation of most of the gene chaperones in almost all the brain regions (Fig. 6). Interestingly, the cerebellum and parietal lobe displayed up-regulation of all the molecular chaperones when treated with ADNP-8 peptide (group B). Therefore, we hypothesize that the up-regulation of the majority of the molecular chaperones in our baseline study may indicate a protective and/or adaptive response of the ER response during sleep deprivation in an attempt to reach cellular homeostasis. Similarly, we hypothesize that the observed gene down-regulation during the peptide treatment experiment may indicate that the peptides offered a profuse protection to the cell thereby significantly reducing the UPR. Up-regulation of molecular chaperones during sleep deprivation, followed by a down-regulation with sleep recovery, has been observed (30). For instance, in Drosophila brain, levels of heat shock protein activator 5 (HSPA5), also known as BiP, increased three-fold with just three hours of sleep deprivation and return to base levels within 24 h of sleep recovery (30). Interestingly, flies with high levels of BiP had more recovery sleep than flies with normal BiP levels. In contrast, flies with inactive BiP had less recovery sleep than flies with normal BiP (30). The HSPA5, or BiP gene, has been shown to increase with sleep deprivation/extended wakefulness in rat cerebral cortex (31). In addition, HSPA5 is the most abundant chaperone in the ER and key for protein folding, activation of UPR and also participates in the translocation of nascent polypeptide chains into the ER. (32, 33). In our baseline studies, we observed an up-regulation of HSPA5 in all brain regions. Conversely, in the peptide treatment studies a down-regulation of the HSPA5 was observed, suggesting that the peptide treatment may have restored the ER functionality to normal levels and attenuated the adaptive UPR (Fig. 20). Taken together, the ER molecular chaperones response data indicated that sleep deprivation affected most of the tested areas of the brain, with cerebellum being the most affected. In addition, the peptide treatments were effective in restoring ER function showing lesser effect in the cerebellum and parietal lobe (Fig. 20).

4.3. Neuronal cell death in frontal lobe, thalamus and hippocampus

In the present study, neuronal cell death was increased in frontal lobe after 96 h of sleep deprivation in all experimental groups except the SD-ADNP-8 + CNTF-11 (Fig. 11). In addition, the number of apoptotic cells was also increased for the SD-ADNP-8 + CNTF-11, ADNP-8 and WP-control groups (Fig. 12). These results were rather unexpected and might be difficult to fully interpret to an understanding, especially when no significant effect in oxidative stress markers (lipid peroxidation and protein oxidation) were observed in this brain region. Additionally, a significant increase in glutathione peroxidase, an

antioxidant defense indicator, was also observed for this brain region. However, the ER molecular chaperone response investigated had indicated a down-regulation in all the experimental groups. Interestingly, with exception of the HSPB1 and HSPA5 genes, the ER gene down-regulation was even lower in the peptide treatment groups than the HC and WP control groups (Fig. 20). It is also interesting that during our baseline studies, for the most part, the ER molecular chaperone response did not get activated until 96 h sleep deprivation (Fig. 6). Taken together, these results suggest that the frontal cortex is less vulnerable to sleep deprivation, and that the peptide treatments induced cells to some extent to reach an adaptive state where the ER UPR is not activated even after 96 h of sleep deprivation. However, further investigations are needed to elucidate the reason for a higher number of necrotic neurons in all other experimental groups, including the controls.

Consistent with the frontal lobe results, the thalamus also showed a significant increase in neuronal cell death in all experimental groups including the controls after 96 h of sleep deprivation (Fig.17). Interestingly, the number of apoptotic cell death observed was also elevated in HC-control group (Fig 18). However, no differences were observed in oxidative stress response. In addition, the ER response displayed a small up-regulation of five of the nine the molecular chaperones genes including CALR, HSP90B1, HSPA2, HSPA5 and HSPB1 only for the SD-ADNP-8 + CNTF-11 experimental group (Fig. 6). In general, all the other groups showed ER gene down-regulation. Taken together, the results suggest that the peptide treatment is effective against oxidative stress. However, the reason for the high number of necrotic neurons, including the control groups, remain unknown.

The hippocampus is an important part of the brain responsible for learning and memory. This area of the brain is also susceptible to stress. Our studies of the hippocampus tissue revealed a decreased in neuronal cell death after 96 h sleep deprivation for all the experimental groups (Fig. 13), suggesting the effectiveness of the peptide treatment for this brain region. The neuroprotective activity of these peptides have been studied. Previous investigations have suggested that the neuroprotective action of CNTF occurs in different mechanisms including inhibition of glutamate excitotoxicity (43), modulation of glial cells response (44) or activation of neuroprotective signal transduction pathways including the JAK (Janus kinase)/STAT (signal transducer and activator of transcription) pathway (STAT/JAK) (45). In addition, importantly, the NAP peptide portion interacts with tubulin and enhances microtubule assembly (46) to increase neurite outgrowth and to specifically protect neurons and glial cells against severe toxicities (47). In our studies, the combination and individual use of the two peptides resulted in decreased neuronal cell death in the hippocampus. This finding suggests that the positive effect of nasal administered peptide treatments for protecting the brain cells in this brain region may have followed the mechanisms discussed above. In addition, no differences in oxidative stress or antioxidant defenses were found. Furthermore, down-regulation of the ER molecular chaperones in all experimental groups was also observed, suggesting that the peptide treatment might have protected the cells against oxidative damage by providing

protection through inhibition of the polymerization of the microtubules, or microfilaments in the cytoskeleton, activating an unknown signal transduction mechanism. It is known that oxidative stress causes disruption of microfilaments and actin modification during aging (48). Other investigations have demonstrated an interaction of ANDP with microtubules (tubulin), but not with microfilaments (actin) (49). Additional studies have confirmed that the active peptide moiety of ADNP (NAP) interacts with tubulin to enhance cellular protection (47).

The sub-granular zone of the dentate gyrus region within the hippocampus is where the formation of new neurons occurs. Stressful experiences, which elevate the levels of glucocorticoids (corticosterone in rats) and stimulate hippocampal glutamate release, inhibit precursor cell proliferation in the dentate gyrus (50). In our studies, we measured the number of neuronal necrotic and apoptotic cells in the dentate gyrus (Fig. 14 and 16). Although SD-ADNP-8 + CNTF-11 and WP-control group showed a decrease, the SD-CNTF-11 and HC-control group displayed an increase in neuronal cell death. This finding is quite unexpected, since previous investigations have been shown that CNTF promotes differentiation and survival of a range of cell types in the mammalian nervous system (39). We could speculate that our CNTF dose may be too low or the pharmacodynimcs not sufficient to reach the site, since earlier studies show the delivered protective effect is found only when it is released by regional neuronal cells (e.g. microglia close to the event) responding due to neuronal cell injury, activating unknown signaling pathways triggered by the insult or injury. Investigations have found an increase in CNTF mRNA with induction of injury in the Schwann cells of the peripheral nervous system (41). However, it has been also demonstrated that exogenously administered CNTF prevents the death of damaged neurons in several injury models *in vivo* (40). In addition, several studies using animal models have shown that administration of CNTF provides protection following CNS injury, including the ability to support striatal output neurons in a pharmacological model of Huntington's disease (42). Therefore, the reason for the increase in neuronal cell death in the HC-control and CNTF-11 groups remains to be investigated. Conversely, the decrease in neuronal cell death in the SD-ADNP-8 + CNTF-11 group suggest that the synergistic activity of the peptide is effective, where CNTF-11 stimulate neuronal proliferation and ADNP-8 provides neuroprotective activities.

Apoptosis is a physiological process in which selected cells are deleted in a rapid, efficient manner through the signal-induced activation of an intrinsic self-destructive cellular process (51). The apoptotic process is characterized by a decrease in mitochondrial membrane potential, activation of caspases, loss of plasma membrane asymmetry, condensation of the cytoplasm and nucleus, and internucleosomal cleavage of DNA (52). Our studies showed no difference in apoptotic cell death in the hippocampus or dentate gyrus for all experimental groups suggesting that after 96 h of sleep deprivation, the UPR in the ER of the cell has not triggered an apoptotic response. Unfortunately, we did not measure the expression of Bax, a mitochondrial apoptotic inducer, or any proteolytic molecules including activation of caspases to measure the early events of the apoptotic

process. Therefore, based on our immunohistochemistry analysis, we did not see any significant difference in apoptotic cell death in the dentate gyrus or hippocampus.

4.4. Hippocampal neurogenesis and peptide treatment

For many years research has demonstrated that neurogenesis is taking place in parts of the brain including the dentate gyrus of the hippocampus. In addition, it also has been examined how the formation of new neurons and maturation of these neurons has been affected by sleep deprivation. Furthermore, several studies revealed that hippocampus-dependent learning and memory formation is associated with increased cell proliferation and neurogenesis, whereas learning impairment is associated with reduced neurogenesis (53). However, other investigations have discovered that sleep recovery for 8 h following acute sleep deprivation does not normalize cell proliferation (54). These findings suggest that sleep does not directly stimulate neurogenesis, but instead, sleep is essential for other cell biological systems that protect and stimulate neurogenesis. In our studies, we observed a significant increase of new neurons in all experimental groups (Fig. 19) suggesting that the peptide treatment was highly effective in protecting the neuronal cells against sleep deprivation.

Decreases in the production and survival of new DG granule cells have been found in response to a variety of harmful factors including chronic stress and glucocorticoids (55, 56). It has been proposed that effects of prolonged sleep deprivation might be an indirect result of stress and increased levels of stress hormones, particularly glucocorticoids (57). Interestingly, in our studies we observed a significant increase in serum corticosterone in the sleep deprived animals (Fig. 5) and treatment with ADNP-8 and CNTF-11 peptides, reduced the levels of corticosterone (Fig. 10). Although high levels of corticosterone might not be the only factor for the inhibition of hippocampal neurogenesis, collectively, our results suggest that there is a positive correlation between high levels of corticosterone and reduced number of neuron formation. It is reasonable to assume that the generation of new cells and neurons in the adult brain is regulated and affected by a wide variety of molecular factors, including trophic factors, cytokines, hormones and a range of neuromodulators and neurotransmitters (58, 59, and 60). Several of these factors are also affected by deprivation or disruption of sleep and may, therefore, provide a link between insufficient sleep and reductions in hippocampal cell proliferation and/or neurogenesis (61). However, the particular mechanisms of how sleep deprivation affects neurogenesis remain unknown. Further investigations are needed to investigate the mechanistic role of neuropeptides ANDP-8 and CNTF-11 in the reduction of corticosterone and proliferation of new neurons.

5.0. Conclusion

We have investigated the protective effects of ADNP-8 and CNTF-11 peptides in the brain following 96 h of sleep deprivation. Results of these investigations indicated that sleep deprivation did not produce significant changes on oxidative stress markers, this could be

due to the protective effect of UPR in the cell. However, GPx, an antioxidant defense mechanism, was up-regulated in the prefrontal cortex suggesting the effectiveness of this peptide for this particular area of the brain. Surprisingly, an increase in neuronal cell death was detected in the sleep deprived, peptide treatment groups and also in the non-sleep deprive controls. The reason for this incongruity may be that in the sleep deprived group, the cell is significantly activating the UPR to preserve ER functionality; as a consequence, protein translation and folding will significantly slow down cell metabolism, slowing down the normal rate of neuronal cell death in the brain. Conversely, the peptide treatments in the sleep deprived animals are able to restore normal cell metabolism (homeostasis) comparable to the non-sleep deprived control animals resulting in a normal cell death rate.

Another possibility is that the ER was overwhelmed and shutdown the UPR, resulting in down-regulation of the molecular chaperones genes and increase in neuronal cell death in the frontal lobe and thalamus. Therefore, the peptide treatment is able to provide protection only to some regions of the brain, including hippocampus. However, this theory does not explain the increased neuronal cell death in the control groups.

An important part of the brain to be considered is the cerebellum. This brain region is involved no only on motor aspects of the brain but also in nonmotor functions of behavior including tasks associated with attention, executive control, language, working memory, learning, pain, emotion, and addiction through a massive interconnection with the cerebral cortex (cerebro-cerebellar circuity) (62). As consequence, abnormal activity in these circuits could lead not only to motor deficits but also to cognitive, attentional, and affective impairments (62). Even though we did not see any significant increase in oxidative stress markers, our studies demonstrated a major increase on ER response molecular chaperones indicating that the cerebellum is highly affected by sleep deprivation. However, our data also suggested that the peptides treatment were able to activate the ER molecular chaperones activity and that fast activation response might protected the neurons from severe injury and consequently death. Unfortunately, due to time and budget limitation, we did not perform any immunohistochemistry analysis for this brain region to assess neuronal cell death.

Overall, sleep deprivation produces damage to the integrity of the hippocampus, a part of the brain responsible for learning and memory, by inhibiting neurogenesis and possibly the compromise of maturation of the newly formed neurons. This damage to the hippocampus could lead to cognitive deficits and mood disorders. The peptide treatments used in this study demonstrated protection to the hippocampus against neuronal cell death and also stimulated neurogenesis under stress conditions. The findings of the present study provide elements of brain region cellular stress mechanistic analysis that creates the basis for further investigations that may lead to the discovery and application of novel and safe strategies to protect the brain against the damaging effects of stress caused by acute sleep deprivation.

6.0. References

1. Anupama Gopalakrishnan, Li Li Ji, Chiara Cirelli. (2003). Sleep Deprivation and Cellular Responses to Oxidative Stress. Sleep. 27. (1): 27 - 35
2. Reimund E. (1994). The free radical flux theory of sleep. Med Hypotheses. Vol. 43: 231-3.
3. Kaufman D, Kilpatrick L, Hudson RG, Campbell DE, Kaufman A, Douglas SD, et al. (1999). Decreased superoxide production, degranulation, tumor necrosis factor alpha secretion, and CD11b/CD18 receptor expression by adherent monocytes from preterm infants. Clinical and Diagnostic Laboratory Immunology. 6(4): 525–9.
4. Liana Beni-Adani, Illana Gozes, Yoram Cohen, Yaniv Assaf, Ruth A. Steingart, Douglas E. Brenneman, Oded Eizenberg, Victoria Trembolver and Esther Shohami. (2000). Peptide Derived from Activity-Dependent Neuroprotective Protein (ADNP) Ameliorates Injury Response in Closed Head Injury in Mice. The Journal of Pharmacology and Experimental Therapeutics. 296: 57 – 63.
5. Zemlyak I, Sapolsky R, Gozes I. (2009). NAP protects against cytochrome c release: inhibition of the initiation of apoptosis. Eur. J. Pharmacol. 618: 9-14.
6. Busciglio J, Pelsman A, Helguera P, Ashur-Fabian O, Pinhasov A, Brenneman DE, Gozes I. (2007). NAP and ADNF-9 protect normal and Down's syndrome cortical neurons from oxidative damage and apoptosis. Curr. Pharm. Des. 13: 1091-8.
7. Beni-Adani L, Gozes I, Cohen Y, Assaf Y, Steingart RA, Brenneman DE, Eizenberg O, Trembolver V, Shohami E. (2001) A peptide derived from activity-dependent neuroprotective protein (ADNP) ameliorates injury response in closed head injury in mice. J Pharmacol Exp Ther. 296:57-63.
8. Romano J, Beni-Adani L, Nissenbaum OL, Brenneman DE, Shohami E, Gozes I. (2002). A single administration of the peptide NAP induces long-term protective changes against the consequences of head injury: gene Atlas array analysis. J Mol Neurosci. 18:37-45.
9. Emsley JG, Hagg T. (2003). Endogenous and exogenous ciliary neurotrophic factor enhances forebrain neurogenesis in adult mice. Exp. Neurol. 183:.298-310.
10. Thompson CL, Wisor JP, Lee CK, Pathak SD, Gerashchenko D, Smith KA, Fischer SR, Kuan CL, Sunkin SM, Ng LL, Lau C, Hawrylycz M, Jones AR, Kilduff TS, Lein ES. (2010) Molecular and anatomical signatures of sleep deprivation in the mouse brain. Front Neurosci 4: Article # 165.
11. Uguz AC, Naziroglu M, Espino J, Bejarano I, González D, Rodríguez AB, Pariente JA (November 2009). Selenium Modulates Oxidative Stress-Induced Cell Apoptosis in Human Myeloid HL-60 Cells Through Regulationof Calcium Release and Caspase-3 and -9 Activities. J Membrane Biol 232: 15-23.

12. Garcia P, Youssef I, Utvik JK, Florent-Béchard S, Barthélémy V, Malaplate-Armand C, Kriem B, Stenger C, Koziel V, Olivier JL, Escanye MC, Hanse M, Allouche A, Desbène C, Yen FT, Bjerkvig R, Oster T, Niclou SP, Pillot T. (2010) Ciliary neurotrophic factor cell-based delivery prevents synaptic impairment and improves memory in mouse models of Alzheimer's disease. J Neurosci. 30:7516-27.
13. Blanchard J, Wanka L, Tung YC, Cárdenas-Aguayo Mdel C, LaFerla FM, Iqbal K, Grundke-Iqbal I. (2010) Pharmacologic reversal of neurogenic and neuroplastic abnormalities and cognitive impairments without affecting Aβ and tau pathologies in 3xTg-AD mice. Acta Neuropathol 120:605-21
14. Blanchard J, Chohan MO, Li B, Liu F, Iqbal K, Grundke-Iqbal I. (2010) Beneficial effect of a CNTF tetrapeptide on adult hippocampal neurogenesis, neuronal plasticity, and spatial memory in mice. J Alzheimers Dis 21:1185-95.
15. Gozes I, Morimoto BH, Tiong J, Fox A, Sutherland K, Dangoor D, Holser-Cochav M, Vered K, Newton P, Aisen PS, Matsuoka Y, van Dyck CH, Thal L. (2005) NAP: research and devel-opment of a peptide derived from activity-dependent neuroprotective protein (ADNP). CNS Drug Rev. 11:353-68.
16. Carol A. Everson, Christa D. Laatsch, and Neil Hogg. (2004). Antioxidant defense responses to sleep loss and sleep recovery. Am J Physiol Regul Integr Comp Physiol 288: R374–R383.
17. Ramanathan L, Gulyani S, Nienhuis R, and Siegel JM. (2002). Sleep deprivation decreases superoxide dismutase activity in rat hippocampus and brainstem. Neuroreport 13: 1387–1390.
18. Gutteridge JM and Halliwell B. (2000). Free radicals and antioxidants in the year 2000. A historical look to the future. Ann NY Acad Sci. 899: 136 – 147.
19. Gopalakrishnan A, Ji Li, Cirelli C. (2003). Sleep deprivation and cellular responses to oxidative stress. Sleep, Vol. 27, No. 1.
20. Vollert C, Zagaara M, Hovattab I, Tanejaa M, Vua A, Daoa A, Levinea A, Alkadhia K, Salim S. (2011). Exercise prevents sleep deprivation-associated anxiety-like behavior in rats: Potential role of oxidative stress mechanisms. Behavioral Brain Research. 224: 233 – 240.
21. D'Almeida V, Lobo LL, Hippolide DC, de Oliveira AC, Nobrega JN, Tufik S. (1998). Sleep deprivation induces brain region-specific decrease in glutathione levels. Neuroreport 9:2853–6.
22. Singh R Kiloung, Singh S. Sharma. (2008). Effect of paradoxical sleep deprivation on oxidative stress parameters in brain regions of adult old rats. Biogerontology. 9: 153 -62.
23. Khadrawy YA, Nour NA, Abul Ezz HS. (2011). Effect of oxidative stress induced by paradoxical sleep deprivation on the activities of Na^+, K^+ -ATPase and

acetylcholinesterase in the cortex and hippocampus of rat. Transl Res. 157: 100 – 7.
24. Ramanathan L, Hu S, Frautschy SA, and Siegel JM. (2010). Short term total sleep deprivation in the rat increases antioxidant responses in multiple brain regions without impairing spontaneous alternation behavior. Behav Brain Res. 207(2): 305. 1- 12.
25. Yu BP. (1994). Cellular defences against damage from reactive oxygen species. Physiol Rev. 74: 139 – 162.
26. Damier P, Hirsch EC, Zhang P, Agid Y, Javoy AF. (1993). Glutathione peroxidase, glial cells and Parkinson disease. Neuroscience. 52: 1 – 6.
27. Marklund SL, Westman NG, Lundgren E, Roos G. (1982). Cooper and zinc containing superoxide dismutase, manganese containing superoxide dismutase, catalase and glutathione peroxidase in normal and neoplastic human cells lines and normal tissues. Cancer Res. 42: 1955 – 61.
28. Yunoki M, Kawauchi M, Ukita N. (1998). Acta Neurochir 71: 142–145
29. Walter P and Ron D. (2011). The unfolded protein response: From stress pathway to homeostatic regulation. Science. 334: 1081-1086.
30. Naidoo N, Casiano V, Cater J, Zimmerman J, Pack AI. (2007). A role for the molecular chaperone protein BiP/GRP78 in Drosophila sleep homeostasis. Sleep. 30(5):557–65.
31. Cirelli C, Gutierrez CM, Tononi G. (2004). Extensive and Divergent Effects of Sleep and Wakefulness on Brain Gene Expression. Neuron. 41: 35–43.
32. Hamman BD, Hendershot LM, Johnson AE. (1998). BiP maintains the permeability barrier of the ER membrane by sealing the lumenal end of the translocon pore before and early in translocation. Cell. 92(6):747–58.
33. Zhang K, Kaufman RJ. (2006). The unfolded protein response: a stress signaling pathway critical for health and disease. Neurology. 66 (2 Suppl 1): S102–9.
34. Butterfield D A, Stadtman E R. (1997). Protein oxidation processes in aging brain. Adv. Cell Aging Gerontol. 2:161–191.
35. Hensley K, Hall N C, Subramaniam R, Cole P, Harris, M, Aksenov M, Aksenova M, Gabbita S P, Wu J F, Carney J M, Lovell, M, Markesbery W R, Butterfield D A. (1995). Brain regional correspondence between Alzheimer's disease histopathology and biomarkers of protein oxidation. J. Neurochem. 65:2146–2156.
36. Lyras L, Cairns N J, Jenner A, Jenner P, Halliwell B. (1997). An assessment of oxidative damage to proteins, lipids, and DNA in brains from patients with Alzheimer's disease. J. Neurochem. 68:2061–2069.
37. Kato K, Kurobe N, Suzuki F, Morishita R, Asano T, Sato T, Inagaki T. (1991). Concentrations of several proteins characteristic of nervous tissue in cerebral cortex of patients with Alzheimer's disease. J. Mol. Neurosci. 3:95–99.

38. Richardson J S. (1993). Free radicals in the genesis of Alzheimer's disease. Ann. N.Y. Acad. Sci. 695:73–76.
39. Richardson P. M. (1994). Ciliary neurotrophic factor: a review. Pharmacol Ther 63(2): 187-98.
40. Hagg T. and S. Varon (1993). Ciliary neurotrophic factor prevents degeneration of adult rat substantia nigra dopaminergic neurons in vivo. Proc Natl Acad Sci U S A 90(13): 6315-6319.
41. Friedman B., S. S. Scherer. (1992). Regulation of ciliary neurotrophic factor expression in myelin-related Schwann cells in vivo. Neuron 9(2): 295-305.
42. Anderson K. D., N. Panayotatos. (1996). Ciliary neurotrophic factor protects striatal output neurons in an animal model of Huntington disease. Proc Natl Acad Sci USA 93(14): 7346-51.
43. Honjo M, Tanihara H, Kido N, Inatani M, Okazaki K, Honda Y. (2000). Expression of ciliary neurotrophic factor activated by retinal Muller cells in eyes with NMDA and kainic acid induced neuronal death. Invest Ophthalmol Vis Sci 41: 552–560.
44. Monville C, Coulpier M, Conti L, De Fraja C, Dreyfus P, Fages C, Riche D, Tardy M, Cattaneo E, Peschanski M. (2001). Ciliary neurotrophic factor may activate mature astrocytes via binding with the leukemia inhibitory factor receptor. Mol Cell Neurosci 17: 373–384.
45. B.A. van Adel, J.M. Arnold, J. Phipps, L.C. Doering, A.K. Ball. (2005). Ciliary Neurotrophic Factor Protects Retinal Ganglion Cells from Axotomy-Induced Apoptosis via Modulation of Retinal Glia In Vivo. J Neurobiol 63: 215–234.
46. Divinski I, Holtser-Cochav M, Vulih-Schultzman I, Steingart RA, and Gozes I. (2006). Peptide neuroprotection through specific interaction with brain tubulin. J Neurochem 98: 973–984.
47. Divinski I, Mittelman L, and Gozes I. (2004). A femtomolar acting octapeptide interacts with tubulin and protects astrocytes against zinc intoxication. J Biol Chem 279: 28531–28538.
48. Dalle-Donne, I. et al. (2001). The actin cytoskeleton response to oxidants: from small heat shock protein phosphorylation to changes in the redox state of actin itself. Free Radic. Biol. Med. 31: 1624–1632.
49. Furman S, Steingart R A, Mandel S, Hauser J M, Brenneman D E, and Gozes I. (2004). Subcellular localization and secretion of activity-dependent neuroprotective protein in astrocytes. Neuron Glia Biol. 1(3): 193–199.
50. Gould E, McEwen BS, Tanapat P, Galea LA, Fuchs E. (1997). Neurogenesis in the dentate gyrus of the adult tree shrew is regulated by psychosocial stress and NMDA receptor activation. J Neurosci. 17:.2492–2498.
51. Qian H, D B, Hausman et al. (2001). TNFalpha induces and insulin inhibits caspase 3 dependent adipocyte apoptosis. Biochem Biophys Res Commun. 284(5): 1176-83.

52. Gullicksen PS, RG. Dean et al. (2004). Detection of DNA fragmentation and apoptotic proteins, and quantification of uncoupling protein expression by real-time RT-PCR in adipose tissue. J Biochem Biophys Methods. 58(1): 1-13.
53. Leuner B, Gould E, Shors T. (2006). Is there a link between adult neurogenesis and learning? Hippocampus 2006. 16: 216–24.
54. Tung A, Takase L, Fornal C, Jacobs B. (2005). Effects of sleep deprivation and recovery sleep upon cell proliferation in adult rat dentate gyrus. Neuroscience. 134: 721–3.
55. Gould E, Tanapat P. Stress and hippocampal neurogenesis. (1999). Biol Psychiatry 46:1472–9.
56. Joels M, Karst H, Krugers HJ, Lucassen P. (2007). Chronic stress: implications for neuronal morphology, function and neurogenesis. Front Neuroendocrinol. 28:72–96.
57. Mirescu C, Peters JD, Noiman L, Gould E. (2006). Sleep deprivation inhibits adult neurogenesis in the hippocampus by elevating glucocorticoids. Proc Natl Acad Sci U S A. 103:19170–5.
58. Abrous DN, Koehl M, Le Moal M. (2005). Adult neurogenesis: from precursors to network and physiology. Physiol Rev. 85:523–69.
59. Ming G, Song H. (2005). Adult neurogenesis in the mammalian central nervous system. Annu Rev Neurosci. 28:223–50.
60. Hagg T. (20050. Molecular regulation of adult CNS neurogenesis: an integrated review. Trends Neurosci. 28:589–95.
61. Meerlo P, Mistlberger RE, Jacobs BL, Heller HC, McGinty D. (2009). New neurons in the adult brain: The role of sleep and consequences of sleep loss. Sleep Medicine Reviews 13: 187–194.
62. Peter L. Strick, Richard P. Dum, and Julie A. Fiez. (2009). Cerebellum and Nonmotor Function. Annu. Rev. Neurosci. 32: 413–34.